

Diese Arbeit wurde vorgelegt am
Lehr- und Forschungsgebiet Theorie der hybriden Systeme

**Komplett autarke Stromversorgung von Kommunen
mittels virtueller erneuerbarer Kraftwerke**
**Complete self-sufficient power supply of counties using
virtual renewable power plants**

Bachelorarbeit
Informatik

Dezember 2020

Vorgelegt von
Presented by

Frederick Lockemann
Bismarckstraße 21A
52066 Aachen
Matrikelnummer: 381204
frederick.lockemann@rwth-aachen.de

Erstprüfer
First examiner

Prof. Dr. rer. nat. Erika Ábrahám
Lehr- und Forschungsgebiet: Theorie der hybriden Systeme
RWTH Aachen University

Zweitprüfer
Second examiner

Prof. Dr. rer. nat. Thomas Noll
Lehr- und Forschungsgebiet: Software Modellierung und Verifikation
RWTH Aachen University

Externer Betreuer
External supervisor

Dr. rer. nat. Pascal Richter
Steinbuch Centre for Computing
Karlsruhe Institute of Technology

Eigenständigkeitserklärung

Hiermit versichere ich, dass ich diese Bachelorarbeit selbstständig verfasst und keine anderen als die angegebenen Quellen und Hilfsmittel benutzt habe. Die Stellen meiner Arbeit, die dem Wortlaut oder dem Sinn nach anderen Werken entnommen sind, habe ich in jedem Fall unter Angabe der Quelle als Entlehnung kenntlich gemacht. Dasselbe gilt sinngemäß für Tabellen und Abbildungen. Diese Arbeit hat in dieser oder einer ähnlichen Form noch nicht im Rahmen einer anderen Prüfung vorgelegen.

Aachen, im Dezember 2020

Frederick Lockemann

Contents

1	Introduction	1
1.1	Related Work	2
1.2	Outline	3
2	Models	3
2.1	County area	6
2.2	Storage Systems	7
2.2.1	Power-To-Gas	7
2.2.2	Pumped-storage hydropower	9
2.2.3	Biogas	11
2.3	Renewable Power Plants	13
2.3.1	Hydropower plant	13
2.3.2	Wind turbines	14
2.3.3	Photovoltaic plant	16
2.4	External electricity	19
2.5	Economic Model	20
3	Control Strategy	21
3.1	Baseline Strategy	21
3.2	Linear programming strategy	23
4	Case Studies	25
4.1	Time horizon analysis	26
4.2	Layout Optimization	31
4.3	Autarky analysis for Herzogenrath	32
4.4	Autarky analysis for Herzogenrath using hydro subsystems	40
4.5	Discussion of the results	43
5	Conclusion and Future Work	45
References		47

1 Introduction

In recent years there has been a rapid increase in global temperatures. This resulted in the last five years to be the warmest compared against the average temperature calculated 1850[9, 22].

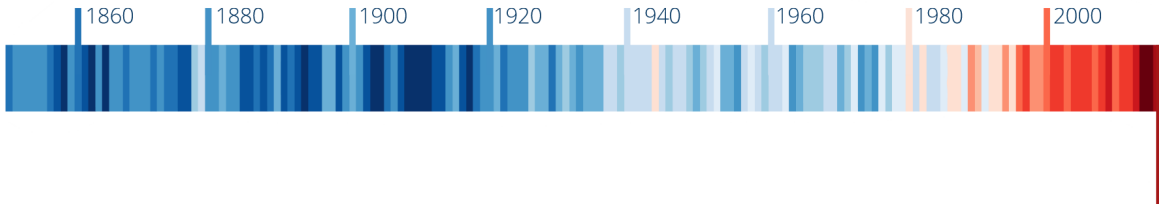


Figure 1: Image from scientists for future. Shown are temperatures of the years 1850 to 2018 compared to the average temperature. The darker the colour the greater the deviation from the average.¹

The temperature increase due to the global climate change is caused by changes in atmospheric composition. Electrical energy use is understood to be the main cause of these changes [16]. In order to approach this issue the German government plans to have every German coal power plant shut down by 2035 [10]. Disconnecting coal power plants from the electric grid would create a deficit in the energy market. A solution for that is presented by renewable energy sources such as wind, solar and hydro. The sun is delivering terawatts of energy to the earth, of which only small fractions would be enough to meet the energy demand of mankind [3]. However the sun is not shining at any given time, causing the need to harness other energy sources to ensure a more diverse power output.

The main problem with renewable energy sources is the unstable power production. Sometimes, these power plants output a lot, at other times no electricity is produced. This creates the need for storage systems which store energy at times where there is an abundance of electricity produced for times where there is not. Many different storage systems like pumped-storage hydropower or power-to-gas systems already exist fulfilling these characteristics. Another storage system harvests energy from biological matter which has to be manually added to the storage. Anaerobic microorganisms convert it into methane gas that can be stored over a long period of time.

Although reforming the energy production is a necessary step towards tackling climate change, it is paramount to make all energy related systems more efficient. Cities consume 75% of the produced energy while producing 80% of greenhouse gas emissions [18]. Hence, cities must become more sustainable. The virtual power plant concept presents a way to optimize the usage of available and new resources by forming a micro grid [19]. It is a dense local electricity grid integrating distributed generators such as wind power plants or photovoltaic power plants and storages. Moving production and consumption closer together has a multitude of advantages for consumers and operators

¹<https://www.scientists4future.org/wp-content/uploads/2019/05/s4f-warming-stripes.png>

alike [12]. Consumers profit from the reductions of emissions and voltage drops and an increase of reliability, which can result in an overall lower price. An advantage for the operator is that micro grids work on low and medium voltage ranges, thus making network infrastructure for high voltages obsolete. Lower investment costs are the consequence.

Considering all the advantages mentioned above, this work will develop an electricity model for a virtual power plant as a micro grid and only harvesting energy from renewable energy sources. This model is called the virtual renewable power plant.

A control strategy is used to control the virtual renewable power plant.

Later in this work two strategies are proposed of which one uses linear programming. Furthermore, the strategy that generates the most revenue given a sample virtual renewable power plant is chosen for the presented case studies.

Finally, the layout optimization is introduced, which finds the best virtual renewable power plant sizing given multiple different use cases. This way the virtual renewable power plant can be optimized to reach a certain degree of self-sufficient power supply. This degree of self-sufficiency refers to the amount of hours in year in which electricity was bought.

1.1 Related Work

In this section the current state-of-the art will be presented regarding virtual power plants and their modelling.

Lombardi et al. [19] state that virtual power plants consist of two main parts. The power production or dispersed generator units and the consumer. Lombardi et al. developed a virtual power plant that closely resembles the concept discussed in this work. Their work focusses on the optimal control of a virtual power plant. Proposed in their work was a model, that consisted on one hand of renewable energy production and a conventional power plant on the energy production side. On the other hand the consumer side consisted of a city, external boiler and industrial complex. Contrary to this work, Lombardi et al. did not consider an energy storage of any kind. Instead they used the additional energy in their model in an Electrolyser plant for Hydrogen production and in a desalination plant to create drinkable water for the city.

Since their virtual power plant uses both conventional and renewable energy to produce electricity, it has certain problems. Most notably, that the renewable resources are not entirely predictable. Therefore a conventional power plant is needed to compensate for that. This work however does not consider any conventional power plants in the micro grid.

Kuzle et al. [17] used a similar model. Here, the virtual power plant is wind and solar power plant combined with a conventional power plant. They however optimized the cost the conventional power plant creates in relation to the rest of the virtual power plant with mixed-integer linear programming in their case study. The goal was to research the influence of the technical minimum of the conventional power plant. Their cases consisted of differing energy production levels from the renewable energy sources. Accordingly they concluded that the higher the technical minimum the higher

are the production costs.

In a second paper the research group focusses on optimizing the revenue of a given virtual power plant in a two-case case study [23]. In the first case the forecast for the energy production of the renewable energy sources are 100% accurate, whereas in the second case the accuracy was only 60%. Both cases considered bilateral contracts for the virtual power plant owner, this means in times in which the energy production cost exceeds the market price, the virtual power plant is able to buy electricity from the grid to meet the minimal required energy amount it is contracted to deliver.

Zdrilić et al. [23] concluded that the usage of the conventional power plant only depends on the relation between production costs and market prices Furthermore, it is clear that the reduced accuracy of the forecast drastically reduced the profit of the power plant.

In contrast to all of the above mentioned works Giuntoli et al. [11] considered energy storage in their model. The ambition of their work is to optimize the net daily profit of the power plant, consisting of thermal and electric generators. They developed a detailed model and evaluated the proposed linear programming algorithm in a case study. They concluded that their proposed approach seems to be flexible and suitable for the virtual power plant's control.

This work however, aims to optimize the virtual renewable power plant towards a complete self-sufficient power supply for counties. To the knowledge of the author no previous work researched this issue.

1.2 Outline

In this work a so-called virtual renewable power plant model which forms a micro grid is designed. It is a power flow model, whose main consumer is the county area.

The following Section 2 focusses on introducing the subsystems making up the virtual renewable power plant and presents the models for these subsystems. Then the economic model is proposed to evaluate a given virtual renewable power plant using different metrics. In Section 3.2 two control strategies are proposed to assign the power flows in the micro grid. Of these two strategies one serves as baseline, against which the second, the linear programming strategy is compared. Section 4 firstly shows that the linear programming strategy is the most optimal compared to the baseline strategy. Additionally, the layout optimization is introduced and multiple case studies for the layout optimization are presented.

2 Models

In this Section the model of the virtual renewable power plant will be proposed to be used further in Sections 3 and 4. The first subsystem is the county area, which is the area of a city with residential, industrial and commercial areas. All of these three areas have in common that they consume electricity and therefore, in the scope of this work, the county area only refers to all buildings that consume only electricity.

Producing electricity is therefore left to the renewable energy power plants, which must be incorporated into the micro grid to profit from the advantages mentioned above. There are different renewable energy sources like solar, wind and hydro energy. However not all energy sources are available at any given location, which is close enough to satisfy proximity constraints for them to be considered part of the virtual renewable power plant. For hydro energy it is necessary, for it to be considered, to have a sufficiently large river or lake close.

For the use of renewable energy sources the biggest challenge is their fluctuating availability. Sometimes the energy output peaks for multiple hours a day, for example with solar power plants on a sunny day, whereas on cloudy days the power output is significantly lower. Consequently, it is paramount to store the energy during times where an abundance of electricity is produced. This way the stored energy can be used to compensate for moments in which the system has an electricity deficiency. This can be done on a plant level, which is common in concentrated solar power plants, or on a micro grid level. In the micro grid electricity of any origin can be stored for a large period of time.

Generally in this work two methods are considered. One of those methods is the power-to-gas technology [15]. It is used to convert electrical energy to hydrogen, which is converted into methane, which in part can be stored and later used in gas power plants to produce electricity. A major advantage this technology provides is its that it is independency from the location it is used in, different from the pumped-storage hydroelectricity method [21]. It relies on two water reservoirs close to each other, of which one must be higher than the other. Here electrical energy is converted into potential energy in contrast to the power-to-gas method, in which it is converted into chemical energy.

Besides another storage system is the biogas storage [20]. In this storage system no surplus electricity is stored because the energy comes from external sources. Agricultural waste, manure, or plant material is converted into methane by anaerobic microorganisms. This methane can be stored over a long period of time. A gas turbine is then used to convert the chemical energy of the methane into electric energy, similar to the process in the power-to-gas storage.

As mentioned earlier this work aims to optimize the later proposed model in different ways. In all cases the virtual renewable power plant must be connected to the state-wide electrical grid. This stems from the fact that in order to generate revenue electricity must be sold, where the only customer is the state-wide electrical grid. Other cases involve the constraint to only meet a certain percentage of renewable energy at any given time. The state-wide electrical grid is considered a subsystem of the virtual renewable power plant, however it is not subject to layout optimizations.

An overview of the virtual renewable power plant can be seen in Figure 2. In the centre of this model is the decision node. It assigns the power flows, these decision variables are shown in blue. All other variables are subject to external influences.

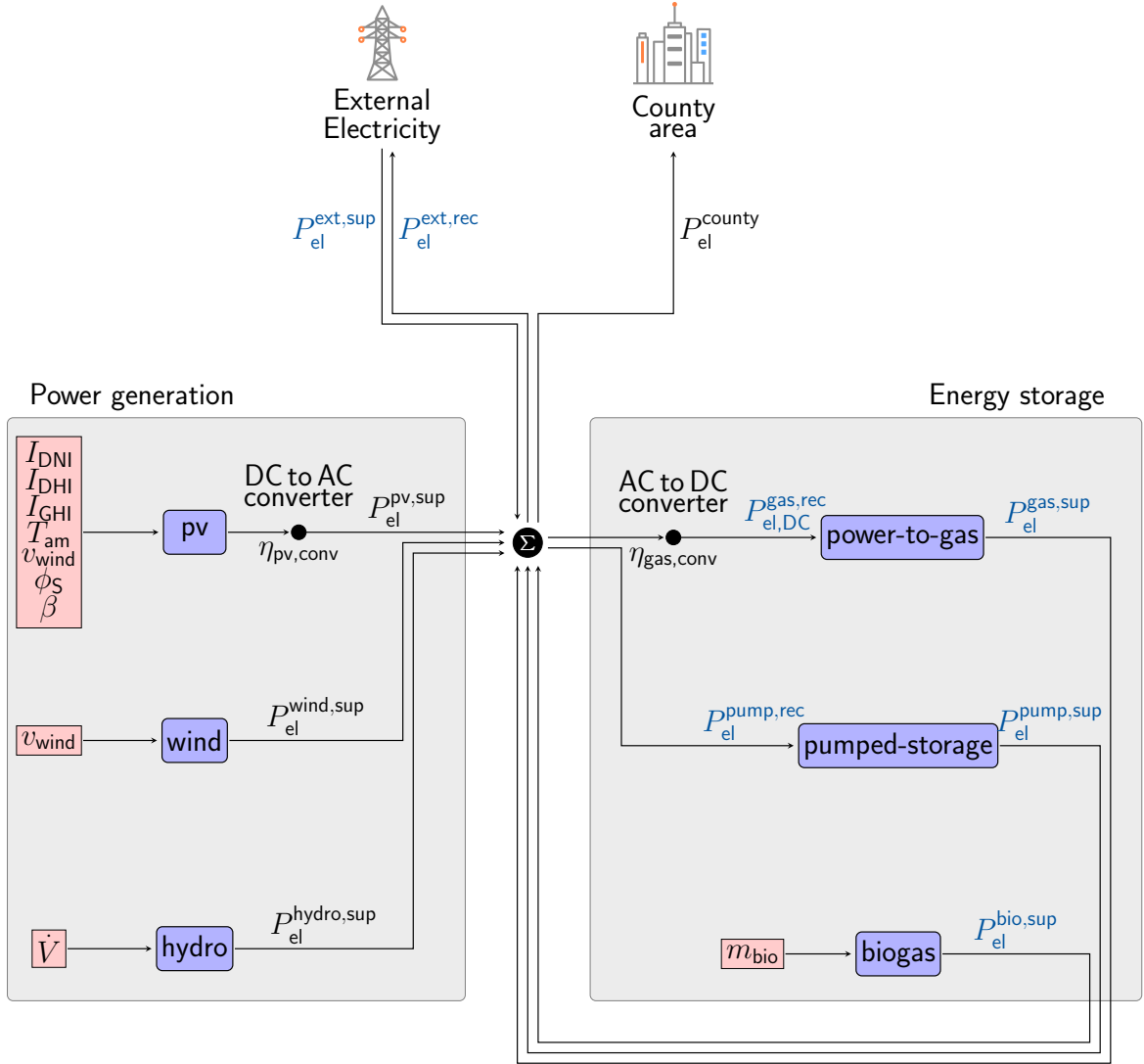


Figure 2: Presented are the electric power flows in the overall model. Blue variables are assigned by the decision node, black variables are considered to be given at any time step. The variables in the red boxes are external inputs.

In the following sections the subsystems are presented. The order is determined in clock-wise fashion by Figure 2 beginning with the county area. In Section 2.1 the model of the county area will be introduced followed by the Storage Systems in Section 2.2 and divided into the power-to-gas and pumped storage system as well as the biogas storage. Then renewable energy plants in Section 2.3 are introduced. The Section is divided into the hydro power, wind and photovoltaic plant. Lastly, the electrical grid is presented in Section 2.4 followed by the economic model in Section 2.5.

2.1 County area

In this section the model for the county area is presented. The power demand is dependent on the demand of commercial, industrial and residential areas and for simplicity reasons this work will be considering a demand curve for these areas together. In Figure 3 a black box model is shown.

As mentioned the model of the county area outputs its time dependent electric demands as a curve and it has no input. An excerpt of such a demand curve can be seen in Figure 4.

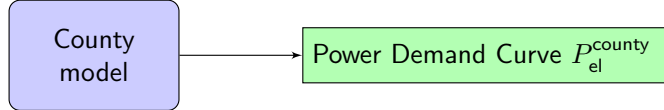


Figure 3: Black box model for the county area. The output is shown in green.

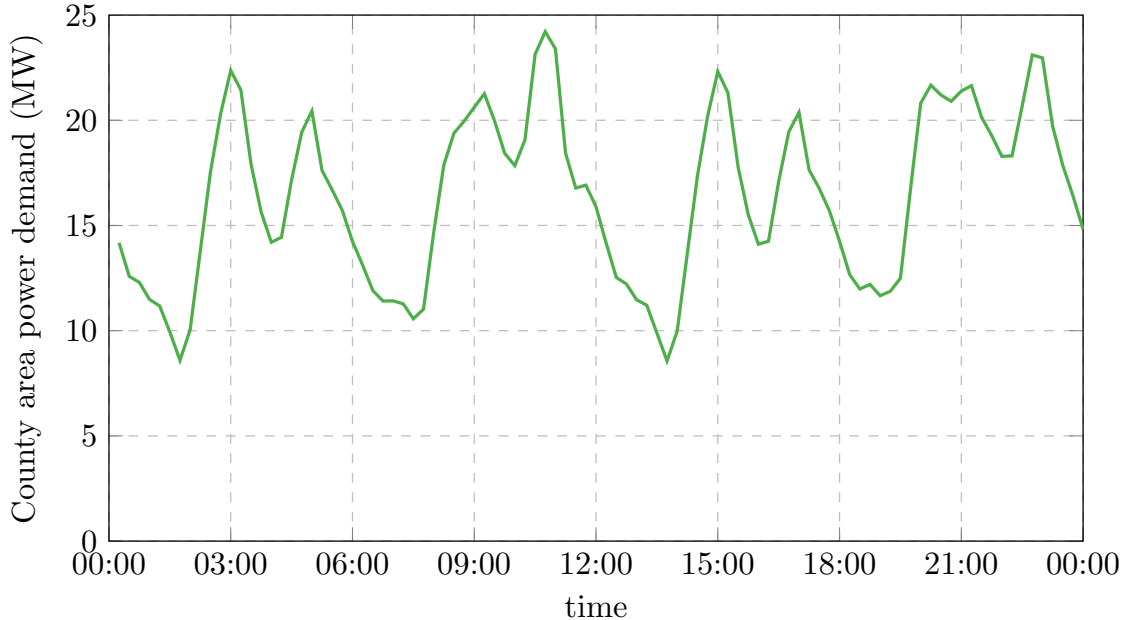


Figure 4: Power curve excerpt of Herzogenrath on January 1st 2016. The power consumption was measured every 15 Minutes.

Category	Description	Abbr.	Units
Output	Power demand curve	P_{el}^{county}	MW

Table 1: Variables of the county area

2.2 Storage Systems

Storage systems are of vast importance in the context of virtual renewable power plants that only rely on renewable energy sources. They create the possibility to store the energy for times in which the power plants harvesting energy from renewable sources do not output sufficient power. As stated in the beginning of Section 2 this work will consider three methods of energy storage, namely power-to-gas, pumped-storage hydropower and the biogas storage method.

2.2.1 Power-To-Gas

The power-to-gas system converts electrical energy in the form of direct current into chemical energy. The particular model used in this work is modelled after one from Jentsch et al. [15].

The process consists of two steps. In the first step electrolysis is used to split water (H_2O) into oxygen (O_2) and hydrogen (H_2). Hydrogen is then used in the second step, the methanation, with carbon dioxide (CO_2) to produce methane (CH_4). The methane can then be used in the natural gas network, or in the case of this work, in a gas turbine to produce electricity. An overview of the procedure can be seen in Figure 5.

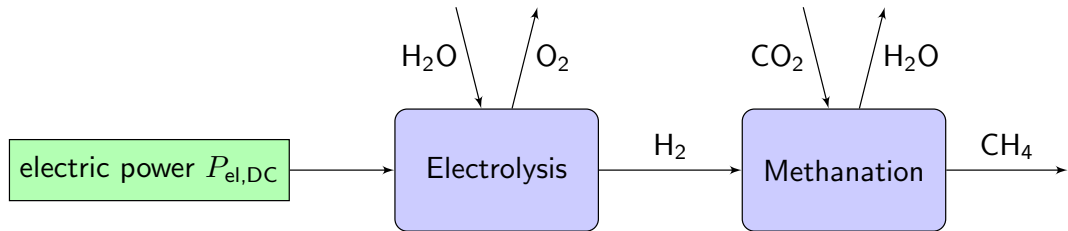


Figure 5: The power-to-gas process combines the electrolysis of water and the methanation of hydrogen and carbon dioxide to produce methane.

In the following it is assumed that the water (H_2O) and carbon dioxide (CO_2) supply is guaranteed and always of sufficient quality. Therefore, for the model of the power-to-gas System, the only input is the excess power. The output is given by how much power is received or supplied from and to the grid.

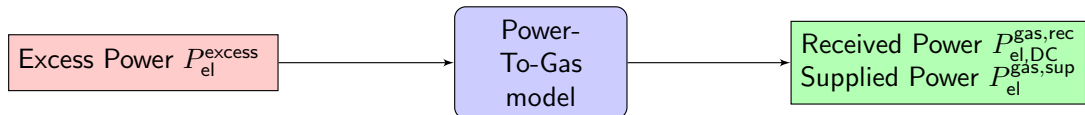


Figure 6: Black box model for the power-to-gas storage. The input is shown in red, the output in green.

$$P_{el}^{gas,sup} = \frac{P_{el}^{gas,gen}}{\eta_{gas,gen}} \quad (1)$$

Equation (1) determines how much power $P_{\text{el}}^{\text{gas,sup}}$ the power-to-gas unit can supply to the grid. Since the gas turbine is ultimately responsible for the conversion from chemical energy into electric energy, it is not loss free. The efficiency with which the chemical energy is converted and therefore electrical energy is generated is given by $\eta_{\text{gas,gen}}$ with $P_{\text{el}}^{\text{gas,gen}}$ being the power taken out of the storage. Furthermore, the supplied power can also be defined as:

$$P_{\text{el}}^{\text{gas,sup}} = f_{\text{gas,pow,sup}} P_{\text{el}}^{\text{gas,sup,max}} \quad (2)$$

$$P_{\text{el,DC}}^{\text{gas,rec}} = f_{\text{gas,pow,rec}} P_{\text{el,DC}}^{\text{gas,rec,max}} \eta_{\text{gas,conv}} \quad (3)$$

Equation (3) determines how power is received by the power-to-gas Unit given by $P_{\text{el,DC}}^{\text{gas,rec}}$. The decision node at the core of the virtual renewable power plant diverts power to storage units based on the control algorithm in use. Therefore, the actual received power is dependent on a power factor $f_{\text{gas,pow,rec}}$ and the highest receivable power $P_{\text{el,DC}}^{\text{gas,rec,max}}$. Since the conversion from alternating to direct current is not perfectly efficient, the losses are given by $\eta_{\text{gas,conv}}$.

$$P_{\text{el}}^{\text{gas,char}} = P_{\text{el,DC}}^{\text{gas,rec}} \eta_{\text{gas,char}} \quad (4)$$

As stated before and given by Figure 5 the conversion from direct current into chemical energy is a twofold procedure. Because it is also subject to thermal and other losses the power ultimately stored is given by $P_{\text{el}}^{\text{gas,char}}$. It is dependent on the power from the AC to DC converter $P_{\text{el,DC}}^{\text{gas,rec}}$ and its efficiency $\eta_{\text{gas,char}}$. Furthermore, the efficiency of the electrolysis and the methanation is given by $\eta_{\text{gas,char}}$.

$$Q_{\text{ch}}^{\text{gas}}(t + \Delta t) = Q_{\text{ch}}^{\text{gas}}(t) + (P_{\text{el}}^{\text{gas,char}}(t) - P_{\text{el}}^{\text{gas,gen}}(t))\Delta t \quad (5)$$

In Equation (5) it is defined how much energy is stored in the power-to-gas storage in the next time step $t + \Delta t$. It depends on the currently stored energy $Q_{\text{ch}}^{\text{gas}}$ and how much the storage was charged or discharged between time step t and $t + \Delta t$ by $P_{\text{el}}^{\text{gas,char}}$ and $P_{\text{el}}^{\text{gas,gen}}$ respectively. All the variables can be seen summarized in Table 2, in which the units are given as well.

Category	Description	Abbr.	Units
Input	Excess power	$P_{\text{el}}^{\text{excess}}$	MW _{el}
Outputs	Received power	$P_{\text{el},\text{DC}}^{\text{gas,rec}}$	MW _{el}
	Supplied power	$P_{\text{el}}^{\text{gas,sup}}$	MW _{el}
Parameters	Storage capacity	$Q_{\text{ch}}^{\text{gas,cap}}$	MW _{ch} h
	Charging efficiency	$\eta_{\text{gas,char}}$	%
	Generating efficiency	$\eta_{\text{gas,gen}}$	%
	Conversion efficiency	$\eta_{\text{gas,conv}}$	%
	Charging power	$P_{\text{el}}^{\text{gas,char}}$	MW _{ch}
	Discharging power	$P_{\text{el}}^{\text{gas,gen}}$	MW _{ch}
	Highest suppliable power	$P_{\text{el}}^{\text{gas,sup,max}}$	MW _{el}
	Highest receivable power	$P_{\text{el},\text{DC}}^{\text{gas,rec,max}}$	MW _{el}
State Variables	Stored energy	$Q_{\text{ch}}^{\text{gas}}$	MW _{ch} h

Table 2: Variables of the power-to-gas storage.

This work does not assume that the model has unlimited monetary resources, therefore for each subsystem the investment cost for building and running cost for operating and maintaining it are presented as well. The investment I^{gas} and C^{gas} are given by the following equations.

$$I^{\text{gas}} = f_{\text{gas},I} Q_{\text{ch}}^{\text{gas,cap}} \quad (6)$$

$$C^{\text{gas}} = f_{\text{gas},C} Q_{\text{ch}}^{\text{gas,cap}} \quad (7)$$

Here the investment and running costs both depend on the capacity $Q_{\text{ch}}^{\text{gas,cap}}$ and respectively a chosen factor for simplicity.

2.2.2 Pumped-storage hydropower

The pumped-storage hydropower is different from the power-to-gas storage for it depends on geological structures. It relies on two water reservoirs at different heights. This storage method converts electricity into potential energy, by pumping water from the lower reservoir into the higher one. Energy can later be converted back into electricity by letting water run through a turbine at the lower reservoir. As mentioned before one disadvantage of this method is its dependency on the location which restricts its usage.

For the following model some assumptions are being made to simplify the model. Firstly, it is assumed that the lower reservoir is larger than the higher one and can hold the entire capacity. Furthermore, it is assumed that both reservoirs are not subject to water evaporation and that the specific weight of the water does not change

over time as well. Lastly, it is assumed that the hydraulic head does not change in the reservoirs.

The pumped-storage hydropower model has the excess power as input and outputs the power it receives or supplies from and to the grid.

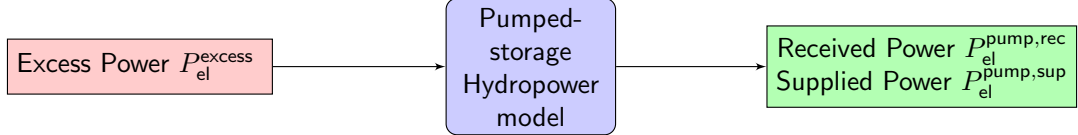


Figure 7: Black box model for the pumped-storage hydropower. The input is shown in red, output in green.

The following equations for generating power and for pumping water into the higher reservoir are taken from Antal et al. [2]. Firstly, the received power is defined:

$$P_{\text{el}}^{\text{pump,rec}} = f_{\text{pump,pow,rec}} P_{\text{el}}^{\text{pump,rec,max}} \quad (8)$$

Indifferent from equation (3) is the dependency of received power on the decision node and consequently on the power factor $f_{\text{pump,pow,rec}}$ and the highest receivable power. However, no AC to DC conversion is necessary, explaining the elimination of a conversion efficiency.

The power with which the pumped-storage storage is being charged is defined as:

$$P_{\text{el}}^{\text{pump,rec}} \eta_{\text{pump,char}} = P_{\text{el}}^{\text{pump,char}} = \gamma \dot{V}_{\text{char}}^{\text{pump}} \Delta H_{\text{pump}} \quad (9)$$

In equation (9) γ stands for the specific weight of the fluid which is in this case water. $\dot{V}_{\text{char}}^{\text{pump}}$ is the flow rate with which the water is pumped into the upper reservoir. ΔH_{pump} refers to the hydraulic head and $\eta_{\text{pump,char}}$ is the efficiency of the pump concerning the conversion of electricity into potential energy.

$$P_{\text{el}}^{\text{pump,sup}} = \frac{P_{\text{el}}^{\text{pump,gen}}}{\eta_{\text{pump,gen}}} = \frac{\gamma \dot{V}_{\text{gen}}^{\text{pump}} \Delta H_{\text{pump}}}{\eta_{\text{pump,gen}}} \quad (10)$$

$\dot{V}_{\text{gen}}^{\text{pump}}$ is the flow rate of the water from the upper reservoir to the lower one. This is considered to be larger than $\dot{V}_{\text{char}}^{\text{pump}}$. $\eta_{\text{pump,gen}}$ is the efficiency of converting the potential energy into electricity. Besides, the alternative definition of $P_{\text{el}}^{\text{pump,sup}}$ is given by:

$$P_{\text{el}}^{\text{pump,sup}} = f_{\text{pump,pow,sup}} P_{\text{el}}^{\text{pump,sup,max}} \quad (11)$$

$$Q_{\text{pot}}^{\text{pump}}(t + \Delta t) = Q_{\text{pot}}^{\text{pump}}(t) + (P_{\text{el}}^{\text{pump,char}}(t) - P_{\text{el}}^{\text{pump,gen}}(t)) \Delta t \quad (12)$$

The stored energy $Q_{\text{pot}}^{\text{pump}}$ in equation (12) is similarly defined to $Q_{\text{ch}}^{\text{gas}}$, but here potential energy is stored. Table 3 again shows all the variables and their corresponding units.

Category	Description	Abbr.	Units
Input	Excess power	$P_{\text{el}}^{\text{excess}}$	MW _{el}
Outputs	Received power	$P_{\text{el}}^{\text{pump,rec}}$	MW _{el}
	Supplied power	$P_{\text{el}}^{\text{pump,sup}}$	MW _{el}
Parameters	Storage capacity	$Q_{\text{pot}}^{\text{pump,cap}}$	MW _{ch} h
	Charging efficiency	$\eta_{\text{pump,char}}$	%
	Discharging efficiency	$\eta_{\text{pump,gen}}$	%
	Charging power	$P_{\text{el}}^{\text{pump,char}}$	MW _{el}
	Discharging power	$P_{\text{el}}^{\text{pump,gen}}$	MW _{el}
	Highest suppliable power	$P_{\text{el}}^{\text{pump,sup,max}}$	MW _{el}
	Highest receivable power	$P_{\text{el}}^{\text{pump,rec,max}}$	MW _{el}
	Generating flow rate	$\dot{V}_{\text{gen}}^{\text{pump}}$	m ³ /s
	Chargin flow rate	$\dot{V}_{\text{char}}^{\text{pump}}$	m ³ /s
	Hydraulic head	ΔH_{pump}	m
State Variables	Stored energy	$Q_{\text{pot}}^{\text{pump}}$	MW _{ch} h

Table 3: Variables of pumped-storage hydropower storage system.

Like in equations (6) and (7) the investment costs I^{pump} and running costs C^{pump} are dependent on the capacity and the respective factor.

$$I^{\text{pump}} = f_{\text{pump},I} Q_{\text{pot}}^{\text{pump,cap}} \quad (13)$$

$$C^{\text{pump}} = f_{\text{pump},C} Q_{\text{pot}}^{\text{pump,cap}}, \quad (14)$$

here the capacity is given by $Q_{\text{pot}}^{\text{pump,cap}}$ and the respective factors for the investment costs and running costs are $f_{\text{pump},I}$ and $f_{\text{pump},C}$.

2.2.3 Biogas

The biogas storage follows a different philosophy than the other two storage systems. With the pumped-storage system the power stored does not come from the virtual renewable power plant. For the biogas storage the energy is from an external source. Agricultural waste, manure and plant material are used to create biogas. This procedure is done by anaerobic microorganisms in an oxygen free environment. These microorganisms break the organic material down and produce methane (CH₄) and

carbon dioxide (CO_2) during the process. This methane, like in the power-to-gas storage, is then burned in a gas turbine to create electricity. A black box model can be seen in Figure 8.

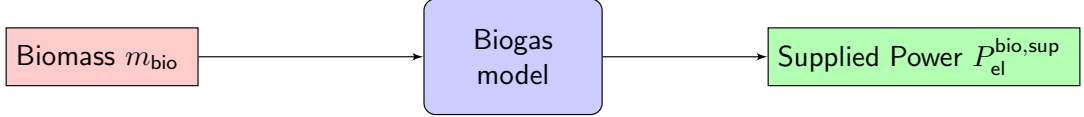


Figure 8: Black box model for the biogas storage system. The input is shown in red, output in green.

There are many different ways to define the yield of methane given the biomass added to the storage tank.

$$Y_{\text{CH}_4} \propto \exp(-\exp(\mu_m)) \quad (15)$$

Zepter et al. [24] define the yield Y_{CH_4} as given in equation (15). μ_m refers to the m^3 biogas per kg volatile solids and day. Volatile solids are solids that can change from the solid state to the gas state rapidly without entering the liquid phase. The exact definition of the methane yield would exceed the scope of this work. Therefore, the yield is defined as a simple linear dependency on the biomass added to the system.

$$Y_{\text{CH}_4} = f_{\text{bio}, Y_{\text{CH}_4}} m_{\text{bio}} \quad (16)$$

The power resulting from the yield is defined as followed.

$$P_{\text{el}}^{\text{bio,char}} = Y_{\text{CH}_4} f_{\text{pow}, Y_{\text{CH}_4}} \quad (17)$$

Since the biogas system stores essentially the same energy medium as the power-to-gas storage - namely methane - the equation for generating power is the same:

$$P_{\text{el}}^{\text{bio,sup}} = \frac{P_{\text{el}}^{\text{bio,gen}}}{\eta_{\text{bio,gen}}} \quad (18)$$

with the alternative definition given by:

$$P_{\text{el}}^{\text{bio,sup}} = f_{\text{bio,pow,sup}} P_{\text{el}}^{\text{bio,sup,max}}. \quad (19)$$

The stored energy by the biogas system can be described as:

$$Q_{\text{ch}}^{\text{bio}}(t + \Delta t) = Q_{\text{ch}}^{\text{bio}}(t) + (P_{\text{el}}^{\text{bio,char}}(t) - P_{\text{el}}^{\text{bio,gen}}(t))\Delta t \quad (20)$$

The variables and their units can be taken from Table 4.

Category	Description	Abbr.	Units
Input	Biomass	m_{bio}	kg
Output	Supplied power	$P_{\text{el}}^{\text{bio,sup}}$	MW _{el}
Parameters	Storage capacity	$Q_{\text{ch}}^{\text{bio,cap}}$	MW _{ch} h
	Generating efficiency	$\eta_{\text{bio,gen}}$	%
	Charging power	$P_{\text{el}}^{\text{bio,char}}$	MW _{ch}
	Discharging power	$P_{\text{el}}^{\text{bio,gen}}$	MW _{ch}
	Highest suppliable power	$P_{\text{el}}^{\text{bio,sup,max}}$	MW _{el}
	Yield factor	$f_{\text{bio},Y_{\text{CH}_4}}$	%
	Yield power factor	$f_{\text{pow},Y_{\text{CH}_4}}$	%
State Variables	Stored energy	$Q_{\text{ch}}^{\text{bio}}$	MW _{ch} h

Table 4: Variables of biogas system.

Finally, the investment costs are proposed.

$$I^{\text{bio}} = f_{\text{bio},I} Q_{\text{ch}}^{\text{bio,cap}} \quad (21)$$

$$C^{\text{bio}} = f_{\text{bio},C} Q_{\text{ch}}^{\text{bio,cap}} \quad (22)$$

The investment I^{bio} and running costs C^{bio} are defined similar to the pumped-storage and power-to-gas storage. They depend in the capacity $Q_{\text{ch}}^{\text{bio,cap}}$ and the respective factor $f_{\text{bio},I}$ and $f_{\text{bio},C}$.

2.3 Renewable Power Plants

Renewable power plants are power plants that convert renewable energy sources into electricity. In this work three of such power plants are presented. In Section 2.3.1 the hydropower plant is presented, followed by the wind power plant in Section 2.3.2. Lastly, the photovoltaic power plant is presented in Section 2.3.3. The hydropower plant differs from other power plants because not every city can use this technology due to the necessity of a moving water body of sufficient size and proximity.

2.3.1 Hydropower plant

Hydropower plants generate power from water that is held up by a dam. The dam serves the purpose of increasing the potential energy of the water by increasing the height. If the dam is opened water will run through pipes converting the potential energy into kinetic energy. The kinetic energy is used to drive the turbine which then generates electric power.

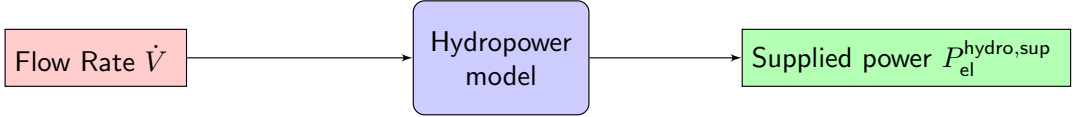


Figure 9: Black box model for the hydropower plant. The input is shown in red, output in green.

The assumptions for the hydropower plant are the same as the ones for the pumped-storage hydropower storage system, namely no water evaporation, no change in the hydraulic head ΔH_{hydro} . Furthermore, the specific weight stays constant γ .

$$P_{\text{el}}^{\text{hydro,sup}}(t) = \eta_{\text{hydro}} \gamma \dot{V} \Delta H_{\text{hydro}} \quad (23)$$

Given the assumptions mentioned above, equation (23) defines the power of the hydropower plant to the virtual power plant $P_{\text{el}}^{\text{hydro,sup}}$. It is structured in the same way as equation (10), therefore no further explanation is necessary. All relevant variables can be taken from Table 5.

Category	Description	Abbr.	Unit
Input	Flow rate	\dot{V}	m^3/s
Output	Supplied power	$P_{\text{el}}^{\text{hydro,sup}}$	MW_{el}
Parameter	Hydraulic head	ΔH_{hydro}	m
	Plant efficiency	η_{hydro}	%

Table 5: Variables of the hydropower plant.

2.3.2 Wind turbines

Wind turbines are a common technology to harvest renewable energy with many types of turbines existing. This makes developing a general model difficult. There are models already developed like one from Feijoo et al. [8]. However, it is more common to use power curves that identify the power output at certain wind speeds. Hence, the wind model in this work has the wind speed as an input and as output the electric power.

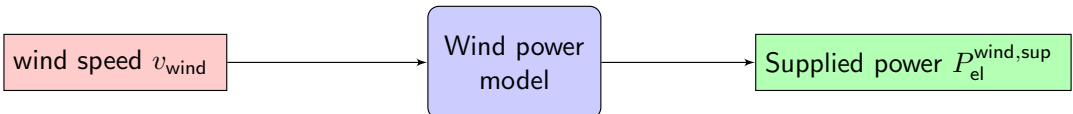


Figure 10: Black box model for the wind plant. The input is shown in red, output in green.

As stated before the power supplied by the power plant to the grid $P_{\text{el}}^{\text{wind,sup}}$ is only defined by the power curve depending on the wind speed $P(v_{\text{wind}})$ and the number of wind turbines N_{turb} in the plant.

$$P_{\text{el}}^{\text{wind,sup}} = N_{\text{turb}} P(v_{\text{wind}}) \quad (24)$$

For the supplied power in equation (24) it is assumed that the wind speed for all turbines is the same and that the efficiency does not decrease if the air is disturbed.

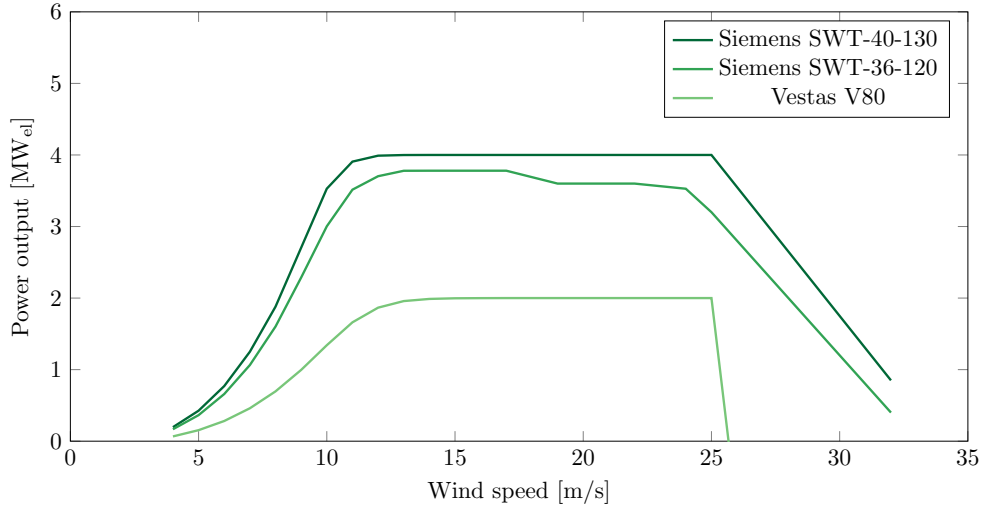


Figure 11: Power curves of three different wind turbines. Each with a cut-in wind speed of 4 m/s and a cut-out wind speed of 25 - 30 m/s.

Category	Description	Abbr.	Units
Input	Wind speed	v_{wind}	m/s
Output	Supplied power	$P_{\text{el}}^{\text{wind,sup}}$	MW _{el}
Parameters	Power Curve	$P(v_{\text{wind}})$	MW _{el}
	Number of turbines	N_{turb}	—

Table 6: Variables of the wind plant.

In the subsystem of the wind turbines the investment costs I^{wind} and running costs C^{wind} only depend on the number of wind turbines N_{turb} .

$$I^{\text{wind}} = f_{\text{wind},I} N_{\text{turb}} \quad (25)$$

$$C^{\text{wind}} = f_{\text{wind},C} N_{\text{turb}} \quad (26)$$

$f_{\text{wind},I}$ is the investment cost per MWh and $f_{\text{wind},C}$ is the running cost per MWh per month.

2.3.3 Photovoltaic plant

The photovoltaic power plant converts the solar irradiance into electricity. The power plant is divided into many photovoltaic collectors, each producing direct current electric power. Since the grid needs the electric power in alternating current; the power plant has an inverter. This work assumes that the photovoltaic panels are fixed in place. The model in the following section is taken from Zhai et al. [25] and Coumbassa [5] and is based on a nominal collector power of 250 W. In Figure 12 the inputs and outputs can be seen for this subsystem.

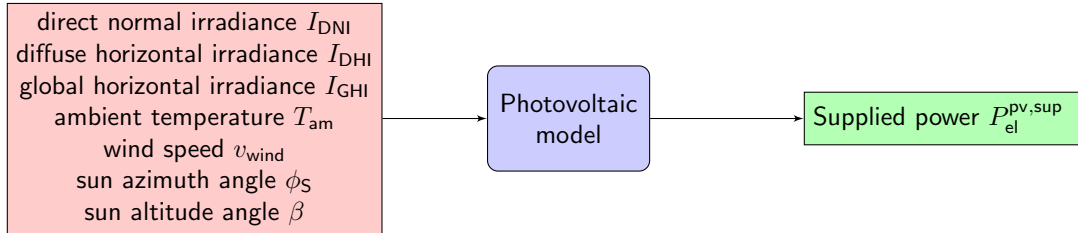


Figure 12: Black box model for the photovoltaic plant. The input is shown in red, output in green.

The photovoltaic panels output the most power if they are at a specific operating temperature $T_{pv,ref}$. Therefore, the current operating temperature has to be calculated.

$$T_{pv} = T_{am} + (T_{nom} - T_{am,nom}) \cdot \frac{I}{I_{nom}} \cdot \frac{U_{nom}}{U} \left[1 - \frac{\eta_{pv,nom}}{\tau\alpha} \right] \quad (27)$$

In equation (28) T_{nom} refers to the nominal operating cell temperature with an ambient temperature $T_{am,nom}$. Furthermore, I_{nom} refers to the nominal solar irradiance and U_{nom} is the rated heat transfer factor with the actual heat transfer factor U is defined as:

$$U = 5.7 + 3.8v_{wind} \quad (28)$$

v_{wind} is the wind speed.

As stated earlier the best power output is dependent on the specific operating temperature and therefore the efficiency is calculated by

$$\eta_{pv} = \eta_{pv,nom} [1 + \gamma (T_{pv} - T_{pv,ref})] \quad (29)$$

with $\eta_{pv,nom}$ being the photovoltaic panels efficiency at nominal temperatures.

Lastly, the direct current power output is defined by:

$$P_{el}^{pv,sup} = N_{pv} A I \eta_{pv} \eta_{pv,conv} f_{pv} \quad (30)$$

A refers to the area of each photovoltaic panel, N_{pv} is the number of panels, $\eta_{pv,conv}$ is the efficiency of converting the direct current into alternating current and f_{pv} is a deration factor for losses caused by soiling of the cover, shading, wiring losses, snow

cover and aging [5]. The total solar irradiance interacting with the panel depends on the setup of the panels. The most important parameters are the tilt angle ψ and the surface azimuth angle ϕ_C . Furthermore, the solar irradiance I consists of a direct beam of solar irradiance I_{BC} , diffuse solar irradiance I_{DC} and the reflected solar irradiance I_{RC} [5]. I is defined as

$$I = I_{BC} + I_{DC} + I_{RC}. \quad (31)$$

Additionally, the I_{BC} depends on the incidence angle θ between the irradiance beam and the collector and the direct normal irradiance I_{DNI} given by

$$I_{BC} = I_{DNI} \cos \theta. \quad (32)$$

The incidence angle used in equation (32) is given by

$$\cos \theta = \cos \beta (\phi_S - \phi_C) \sin \psi + \sin \beta \cos \psi. \quad (33)$$

Furthermore, the solar altitude β depends on the latitude L of the photovoltaic plant, the solar declination angle δ and the hour angle H . The hour angle is the number of degrees the earth must rotate before the sun is directly over the longitude of the photovoltaic plant [5]. β is calculated by

$$\sin \beta = \cos L \cos \delta \cos H + \sin L \sin \delta \quad (34)$$

where δ is given by

$$\delta = 23.45 \sin \left(\frac{360}{365}(n - 81) \right) \quad (35)$$

with n being the number of the current day in the year. The hour angle H is defined as

$$H = (15) \cdot (12 - st) \quad (36)$$

$$st = ct - \frac{\text{longitude}}{15^\circ} + \frac{E}{60} \quad (37)$$

$$E = 9.78 \sin 2B - 7.53 \cos B - 1.5 \sin B \quad (38)$$

$$B = \frac{360}{365}(n - 81), \quad (39)$$

st is the solar time, ct the clock time and again n the number of the current day in the year.

The solar azimuth ϕ_S is defined by

$$\sin \phi_S = \frac{\cos \delta \sin H}{\cos \beta}. \quad (40)$$

Finally, the diffuse irradiance is given by

$$I_{DC} = I_{DHI} \left(\frac{1 + \cos \psi}{2} \right) \quad (41)$$

and the reflected irradiance by

$$I_{RC} = \rho I_{GHI} \left(\frac{1 - \cos \psi}{2} \right) \quad (42)$$

with ρ being the ground reflectance.

All variables and their units for the photovoltaic plant are summarized in Table 7.

Category	Description	Abbr.	Units
Inputs	Direct normal irradiance	I_{DNI}	W/m^2
	Diffuse horizontal irradiance	I_{DHI}	W/m^2
	Global horizontal irradiance	I_{GHI}	W/m^2
	Ambient temperature	T_{am}	$^\circ\text{C}$
	Wind speed	v_{wind}	m/s
	Sun azimuth angle	ϕ_S	$^\circ$
	Sun altitude angle	β	$^\circ$
Output	Supplied power	$P_{el}^{pv,sup}$	MW_{el}
Parameters	Nominal operating cell temperature	T_{nom}	$^\circ\text{C}$
	Ambient temperature for nominal operating cell temperature	$T_{am,nom}$	$^\circ\text{C}$
	Nominal global irradiance	I_{nom}	W/m^2
	Rated heat transfer factor	U_{nom}	—
	Transfer absorption factor	$\tau\alpha$	—
	Nominal efficiency	$\eta_{pv,nom}$	%
	Temperature factor	γ	%/ K
	Module temperature under standard test conditions	$T_{pv,ref}$	$^\circ\text{C}$
	Surface azimuth	ϕ_C	$^\circ$
	Surface area of one collector	A	m^2
	Number of collectors	N_{pv}	—
	Conversion efficiency	$\eta_{pv,conv}$	%
	Tilt angle	ψ	$^\circ$
	Ground reflectance	ρ	—

Table 7: Variables of the photovoltaic plant.

Eventually, the investment I^{pv} and C^{pv} running costs are presented. Both are dependent on the number of panels and surface area of each panel.

$$I^{\text{pv}} = f_{\text{pv},I} N_{\text{pv}} A \quad (43)$$

$$C^{\text{pv}} = f_{\text{pv},C} N_{\text{pv}} A \quad (44)$$

where $f_{\text{pv},I}$ is the investment cost per MWh and $f_{\text{pv},C}$ is the running cost per MWh per month.

2.4 External electricity

In this work the external electricity is the state-wide electrical grid. The aim of this work is to make the energy production independent of the state-wide electrical grid as much as possible. However, if the energy production of the virtual power plant is not sufficient to satisfy the demands of the county area, it is possible to buy electricity from the external electricity grid. This could be the case in times of insufficient weather conditions. Thus the input of the external electrical grid model is the excess power in the virtual renewable power plant with the supplied or received power being outputs.

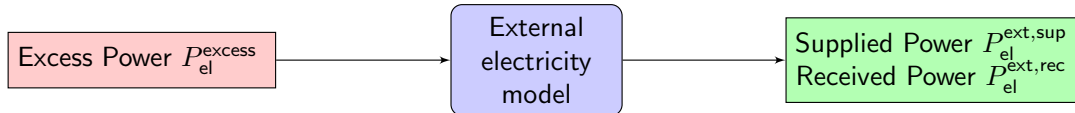


Figure 13: Black box model for the external electricity grid. The input is in red, output in green.

Additionally, another assumption about the power supplied and received by the external grid will be made. They are constraint by the respective highest power $P_{\text{el}}^{\text{ext,sup,max}}$ and $P_{\text{el}}^{\text{ext,rec,max}}$.

$$P_{\text{el}}^{\text{ext,sup}} = f_{\text{ext,pow,sup}} P_{\text{el}}^{\text{ext,sup,max}} \quad (45)$$

$$P_{\text{el}}^{\text{ext,rec}} = f_{\text{ext,pow,rec}} \min(P_{\text{el}}^{\text{excess}}, P_{\text{el}}^{\text{ext,rec,max}}) \quad (46)$$

In equations (45) and (46) the amounts of power sold and bought from and to the grid directly are defined. They correspond to the profit made by the virtual renewable power plant and are subject to the control strategy of the decision node. It assigns the values for $f_{\text{ext,pow,sup}}$ and $f_{\text{ext,pow,rec}}$. For the external grid all variables can be taken from Table 8.

Category	Description	Abbr.	Units
Inputs	Excess power	$P_{\text{el}}^{\text{excess}}$	MW _{el}
	Electricity tariff	π	€/MW _{el}
Parameters	Highest Supplied power	$P_{\text{el}}^{\text{ext,sup,max}}$	MW _{el}
	Highest Received power	$P_{\text{el}}^{\text{ext,rec,max}}$	MW _{el}
Outputs	Supplied power	$P_{\text{el}}^{\text{ext,sup}}$	MW _{el}
	Received power	$P_{\text{el}}^{\text{ext,rec}}$	MW _{el}

Table 8: Variables of external electricity grid.

2.5 Economic Model

In this Section the economic model is presented. The overall model is comprised of the revenue from the sold electricity, the running costs of the individual subsystems, the initial investments for building each subsystem and the levelized cost of energy. The investments and running costs were presented before, so firstly the revenue regarding selling and buying electricity is presented. After Coumbassa [5] the revenue depends on the sold and bought electric energy $P_{\text{el}}^{\text{ext,rec}}$ and $P_{\text{el}}^{\text{ext,sup}}$ as well as the electricity tariff π . Additionally, the stored energy is also considered for the revenue at the end of the considered timespan, see Figure 14.



Figure 14: Black box model for the economic model. The inputs are in red, output in green.

The tariffs for buying or selling electricity change over time as does the amount of buying or selling electricity. Therefore, with reference to Coumbassa [5] and Cirocco et al. [4] the revenue from electricity is defined as:

$$R^{\text{el}} = \sum_{t=t_0}^{t_{\text{end}}} \pi(t) P_{\text{el}}^{\text{ext,sup}}(t) \cdot \Delta t - \sum_{t=t_0}^{t_{\text{end}}} \pi(t) P_{\text{el}}^{\text{ext,rec}}(t) \cdot \Delta t + \pi_{\text{res}} Q_{\text{overall}}^{\text{stor}} \quad (47)$$

As mentioned earlier, the stored energy at the end of the considered time is also considered for revenue generation. However, the tariff π_{res} determines how much the virtual power plant is able to sell this energy for.

Another way to analyse the virtual renewable power plant is to calculate the levelized cost of energy (LCOE). The LCOE defines the costs per MW_{el}. This can either be determined over the lifetime N_{lifetime} of the power plant or one year. In the scope of this work, the annual LCOE is used and defined by:

$$LCOE = \frac{C_{\text{Invest}} \cdot \frac{(1+r_{\text{rate}})^{N_{\text{lifetime}} \cdot r_{\text{rate}}}}{(1+r_{\text{rate}})^{N_{\text{lifetime}} - 1}} + C_{\text{O\&M}}}{\left(P_{\text{el}}^{\text{bio,sup}} + P_{\text{el}}^{\text{hydro,sup}} + P_{\text{el}}^{\text{pump,sup}} + P_{\text{el}}^{\text{gas,sup}} + P_{\text{el}}^{\text{pv,sup}} + P_{\text{el}}^{\text{wind,sup}} \right)} \quad (48)$$

C_{Invest} and $C_{\text{O\&M}}$ are the sums over all investments and O&M costs respectively. Besides, r_{rate} is the interest rate.

3 Control Strategy

A control strategy is needed to assign the power flows in the virtual renewable power plant, namely $P_{\text{el}}^{\text{ext,rec}}, P_{\text{el}}^{\text{ext,sup}}, P_{\text{el,DC}}^{\text{gas,rec}}, P_{\text{el}}^{\text{gas,sup}}, P_{\text{el}}^{\text{pump,rec}}, P_{\text{el}}^{\text{pump,sup}}, P_{\text{el}}^{\text{bio,sup}}$. The aim of this control strategy is to maximize the revenue generated over the time period $t \in [t_0, t_{\text{end}}]$, while the time interval is not continuous, but divided with a step size Δt . Furthermore, in this section all storages are completely empty at $t = t_0$. Firstly, in Section 3.1 a baseline strategy is proposed. Later in Section 3.2 a linear program optimization is used to find the most optimal control strategy.

3.1 Baseline Strategy

The baseline strategy ensures that the county areas power demand is met at any given time. Storage systems are only charged if and only if a surplus of power exists in the micro gird of the virtual renewable power plant. As mentioned above the power output of the renewable power plants and power demand of the county area is known in advance. Therefore, the power flows of the renewable power plants are prioritized to supply the county area. Accordingly, the baseline strategy reacts each time step on the relation of the power output to the power demand of the county area. There are two cases given below:

- $P_{\text{el}}^{\text{county}}(t_i) < \left(P_{\text{el}}^{\text{hydro,sup}}(t_i) + P_{\text{el}}^{\text{pv,sup}}(t_i) + P_{\text{el}}^{\text{wind,sup}}(t_i) \right)$
- $P_{\text{el}}^{\text{county}}(t_i) \geq \left(P_{\text{el}}^{\text{hydro,sup}}(t_i) + P_{\text{el}}^{\text{pv,sup}}(t_i) + P_{\text{el}}^{\text{wind,sup}}(t_i) \right)$

The two cases are called surplus and generate mode respectively based on the reaction of the strategy with regards to the power flows from and to the storages. Both cases and the reaction of the reaction to these are described below.

Surplus mode In the surplus mode the first case holds. Therefore, all additional power $P_{\text{el}}^{\text{excess}}(t_i)$ can be utilized for revenue generation or used to be stored. This strategy prioritizes storage over revenue, meaning all additional power is first diverted towards the storage systems. The receivable power must be determined, so that the capacity of the storage is not exceeded. This is shown for the power-to-gas system,

while the pumped-storage hydropower system will be handled similarly.

At first the amount of power that can be added to the storage must be determined:

$$P_{\text{el}}^{\text{pos,gas,rec}}(t_i) = \frac{(Q_{\text{ch}}^{\text{gas,cap}} - Q_{\text{ch}}^{\text{gas}}(t_i))}{\eta_{\text{gas,char}} \eta_{\text{gas,conv}} \Delta t} \quad (49)$$

The actual received power is then determined by:

$$P_{\text{el}}^{\text{gas,rec}}(t_i) = \min \left(P_{\text{el}}^{\text{pos,gas,rec}}(t_i), \frac{P_{\text{el}}^{\text{excess}}(t_i)}{2} \right) \quad (50)$$

$P_{\text{el}}^{\text{excess}}$ is halved, since the other half is diverted to the pumped-storage hydropower system. If the storage systems cannot consume the excess power $P_{\text{el}}^{\text{excess}}$ entirely, the rest is sold to the electrical grid for revenue generation:

$$P_{\text{el}}^{\text{ext,rec}}(t_i) = P_{\text{el}}^{\text{excess}}(t_i) - P_{\text{el}}^{\text{gas,rec}}(t_i) - P_{\text{el}}^{\text{pump,rec}}(t_i) \quad (51)$$

Generate mode For the generate mode the second case given above holds. The storage systems must then compensate the deficiencies of power between the county areas demand and the renewable power plants. In this strategy all storage systems generate power given by the same fraction of the highest suppliable power. This fraction $\hat{f}_{\text{stor,pow,sup}}$ is defined by:

$$\hat{f}_{\text{stor,pow,sup}} = \frac{P_{\text{el}}^{\text{county}}(t_i) - (P_{\text{el}}^{\text{hydro,sup}}(t_i) + P_{\text{el}}^{\text{pv,sup}}(t_i) + P_{\text{el}}^{\text{wind,sup}}(t_i))}{(P_{\text{el}}^{\text{bio,sup,max}}(t_i) + P_{\text{el}}^{\text{pump,sup,max}}(t_i) + P_{\text{el}}^{\text{gas,sup,max}}(t_i))} \quad (52)$$

If the deficiency is greater than the sum of all highest suppliable power, $\hat{f}_{\text{stor,pow,sup}}$ will become greater than one. Hence the final fraction $f_{\text{stor,pow,sup}}$ is defined by:

$$f_{\text{stor,pow,sup}} = \begin{cases} 1 & , \hat{f}_{\text{stor,pow,sup}} > 1 \\ \hat{f}_{\text{stor,pow,sup}} & , \text{else} \end{cases} \quad (53)$$

If the power demand still cannot be satisfied, the electrical grid connected to the virtual renewable power plant must supply the rest. Therefore, the $P_{\text{el}}^{\text{ext,sup}}$ is defined by:

$$\begin{aligned} P_{\text{el}}^{\text{ext,sup}} = & P_{\text{el}}^{\text{county}}(t_i) - (P_{\text{el}}^{\text{hydro,sup}}(t_i) + P_{\text{el}}^{\text{pv,sup}}(t_i) + P_{\text{el}}^{\text{wind,sup}}(t_i)) \\ & - f_{\text{stor,pow,sup}} (P_{\text{el}}^{\text{bio,sup,max}}(t_i) + P_{\text{el}}^{\text{pump,sup,max}}(t_i) + P_{\text{el}}^{\text{gas,sup,max}}(t_i)) \end{aligned} \quad (54)$$

Finally, after ending at $t = t_{\text{end}}$ the strategy is evaluated with equation (48). Other strategies can be compared against this strategy using the same metric.

3.2 Linear programming strategy

The underlying optimization problem can alternatively be solved by formulating it as a linear program (LP). As mentioned above, the time period $t \in [t_0, t_{\text{end}}]$ is divided into N equidistant steps, given by the step size Δt .

For each time step t_i for $i \in [0, \dots, N - 1]$ a horizon window $[t_i, t_{i+k}]$ is used to solve the LP. The window size k of the horizon window determines how many future time steps are being considered to find the optimal assignment for the decision vector. The decision vector includes all the values the control strategy has to assign.

In the following this work uses the notation $P(t_{i+j} | t_i)$, which corresponds to the power at time t_{i+j} that was decided at t_i . For known variables this notation determines the known value at t_{i+j} used to find the assignment at t_i . This leads to the discretized decision vector u :

$$u(t_{i+j} | t_i) = (P_{\text{el}}^{\text{bio,sup}}(t_{i+j} | t_i), P_{\text{el}}^{\text{ext,rec}}(t_{i+j} | t_i), P_{\text{el}}^{\text{ext,sup}}(t_{i+j} | t_i), P_{\text{el}}^{\text{pump,rec}}(t_{i+j} | t_i), \\ P_{\text{el}}^{\text{pump,sup}}(t_{i+j} | t_i), P_{\text{el,DC}}^{\text{gas,rec}}(t_{i+j} | t_i), P_{\text{el}}^{\text{gas,sup}}(t_{i+j} | t_i))^T \quad (55)$$

The objective function defines the goal for the LP. In this work the objective is to maximize the discretized electrical revenue (47) over the time horizon given by:

$$\max_u \sum_{j=0}^k \pi(t_{i+j} | t_i) \cdot P_{\text{el}}^{\text{ext,sup}}(t_{i+j} | t_i) \cdot \Delta t - \\ \sum_{j=0}^k \pi(t_{i+j} | t_i) \cdot P_{\text{el}}^{\text{ext,rec}}(t_{i+j} | t_i) \cdot \Delta t + \pi_{\text{res}} \cdot Q_{\text{overall}}^{\text{stor}}(t_{i+j} | t_i) \quad (56)$$

From Section 2 necessary constraints can be derived and reformulated in a discretized manner. This is done so that they are dependent on the decision vector u for the horizon window $(t_{i+j} | t_i)$:

- Supplied power of the power-to-gas system (2):

$$0 \leq P_{\text{el}}^{\text{gas,sup}}(t_{i+j} | t_i) \leq P_{\text{el}}^{\text{gas,sup,max}}$$

- Received power of the power-to-gas system (4):

$$0 \leq P_{\text{el,DC}}^{\text{gas,rec}}(t_{i+j} | t_i) \leq P_{\text{el,DC}}^{\text{gas,rec,max}} \eta_{\text{gas,conv}}$$

- Stored Energy of the power-to-gas system (5):

$$Q_{\text{ch}}^{\text{gas}}(t_{i+j} | t_{i+1}) = Q_{\text{ch}}^{\text{gas}}(t_{i+j} | t_i) + (P_{\text{el}}^{\text{gas,char}}(t_{i+j} | t_i) - P_{\text{el}}^{\text{gas,gen}}(t_{i+j} | t_i)) \cdot \Delta t$$

- Received power of the pumped-storage hydropower system (8):

$$0 \leq P_{\text{el}}^{\text{pump,rec}}(t_{i+j} | t_i) \leq P_{\text{el}}^{\text{pump,rec,max}}$$

- Supplied power of the pumped-storage hydropower system (11):

$$0 \leq P_{\text{el}}^{\text{pump,sup}}(t_{i+j} | t_i) \leq P_{\text{el}}^{\text{pump,sup,max}}$$

- Stored Energy of the pumped-storage hydropower system (12):

$$Q_{\text{pot}}^{\text{pump}}(t_{i+j} | t_{i+1}) = Q_{\text{pot}}^{\text{pump}}(t_{i+j} | t_i) + (P_{\text{el}}^{\text{pump,char}}(t_{i+j} | t_i) - P_{\text{el}}^{\text{pump,gen}}(t_{i+j} | t_i)) \cdot \Delta t$$

- Supplied power of the biogas system (19):

$$0 \leq P_{\text{el}}^{\text{bio,sup}}(t_{i+j} | t_i) \leq P_{\text{el}}^{\text{bio,sup,max}}$$

- Stored Energy of the biogas system (20):

$$Q_{\text{ch}}^{\text{bio}}(t_{i+j} | t_{i+1}) = Q_{\text{ch}}^{\text{bio}}(t_{i+j} | t_i) + (P_{\text{el}}^{\text{bio,char}}(t_{i+j} | t_i) - P_{\text{el}}^{\text{bio,gen}}(t_{i+j} | t_i)) \cdot \Delta t$$

To ensure that the county area is sufficiently supplied with electricity another constraint must be introduced:

$$\begin{aligned} P_{\text{el}}^{\text{county}}(t_{i+j} | t_i) &\leq P_{\text{el}}^{\text{hydro,sup}}(t_{i+j} | t_i) + P_{\text{el}}^{\text{pv,sup}}(t_{i+j} | t_i) + P_{\text{el}}^{\text{wind,sup}}(t_{i+j} | t_i) \\ &+ P_{\text{el}}^{\text{ext,sup}}(t_{i+j} | t_i) + P_{\text{el}}^{\text{gas,sup}}(t_{i+j} | t_i) \\ &+ P_{\text{el}}^{\text{pump,sup}}(t_{i+j} | t_i) + P_{\text{el}}^{\text{bio,sup}}(t_{i+j} | t_i) \end{aligned}$$

Furthermore, the sum of received power and the sold power must never exceed the difference of the power demand of the county area and the power in the system. Therefore, an additional constraint is defined by:

$$\begin{aligned} P_{\text{el}}^{\text{ext,rec}}(t_{i+j} | t_i) + P_{\text{el,DC}}^{\text{gas,rec}}(t_{i+j} | t_i) + P_{\text{el}}^{\text{pump,rec}}(t_{i+j} | t_i) &\leq \\ (P_{\text{el}}^{\text{hydro,sup}}(t_{i+j} | t_i) + P_{\text{el}}^{\text{pv,sup}}(t_{i+j} | t_i) + P_{\text{el}}^{\text{wind,sup}}(t_{i+j} | t_i) \\ + P_{\text{el}}^{\text{ext,sup}}(t_{i+j} | t_i) + P_{\text{el}}^{\text{gas,sup}}(t_{i+j} | t_i) + P_{\text{el}}^{\text{pump,sup}}(t_{i+j} | t_i) + \\ P_{\text{el}}^{\text{bio,sup}}(t_{i+j} | t_i)) - P_{\text{el}}^{\text{county}}(t_{i+j} | t_i) \end{aligned}$$

Additionally, the power from the power plants and the demand of the county area are given. Thus the decision vector u must be assigned at every time step t_i within the horizon window to fulfil the above mentioned constraints to optimize the results of the objective function. As can be seen from the constraints above, the LP model indeed only depends on linear functions and was optimized using the Gurobi¹ solver.

¹<https://www.gurobi.com/>

4 Case Studies

In this Section the case studies are presented. First, the baseline strategy and the linear programming strategy are compared based on a sample power plant to find the best time horizon. The sample power plants configuration is summarized in Table 9. For meteorological data in this section, the Climate OneBuilding² database, was used for Aachen. The meteorological data includes wind speed, irradiation and temperature for every hour over one year. A visual representation is given in Figures (a) - (e). The biogas storage does not receive any electricity to store, but biological matter to convert to methane. For all upcoming case studies the biogas receives 100 tones of biological matter every twelve hours.

Furthermore, the tariff data from the epex spot market is used [1]. The exact values are presented in Table 10. Additionally, the second optimization searching for the configurations for different scenarios is introduced. It uses the linear programming strategy to decide the power flows and the meteorological data as described above.

Parameter		Value	Optimization
$Q_{\text{ch}}^{\text{bio},\text{cap}}$	Storage capacity	200 MW _{ch} h	○
$\eta_{\text{bio},\text{gen}}$	Generating efficiency	60 %	
$P_{\text{el}}^{\text{bio},\text{sup},\text{max}}$	Highest suppliable power	20 MW _{el}	○
$f_{\text{bio},Y_{\text{CH}_4}}$	Yield factor	55 %	
$f_{\text{pow},Y_{\text{CH}_4}}$	Yield power factor	60 %	
$f_{\text{bio},I}$	Investment factor	3 ,500 €/kW _{el}	
$f_{\text{bio},C}$	Running cost factor	52.5 €/kW _{el}	
$Q_{\text{ch}}^{\text{gas},\text{cap}}$	Storage capacity	300 MW _{ch} h	○
$\eta_{\text{gas},\text{char}}$	Charging efficiency	50 %	
$\eta_{\text{gas},\text{gen}}$	Generating efficiency	50 %	
$P_{\text{el}}^{\text{gas},\text{sup},\text{max}}$	Highest suppliable power	30 MW _{el}	○
$P_{\text{el},\text{DC}}^{\text{gas},\text{rec},\text{max}}$	Highest receivable power	30 MW _{el}	○
$\eta_{\text{gas},\text{conv}}$	Converter efficiency	95 %	
$f_{\text{gas},I}$	Investment factor	3 ,500 €/kW _{el}	
$f_{\text{gas},C}$	Running cost factor	52.5 €/kW _{el}	
	Site of power plant	50.86 °N, 6.08 °E	
T_{nom}	Nominal operating cell temperature	46 °C	
$T_{\text{am,nom}}$	Ambient temperature for nominal operating cell temperature	20 °C	
I_{nom}	Nominal global irradiance	800 W/m ²	

²<http://climate.onebuilding.org/>

Parameter		Value	Optimization
U_{nom}	Rated heat transfer factor	9.5	—
$\tau\alpha$	Transfer absorption factor	0.8	—
$\eta_{\text{pv,nom}}$	Nominal efficiency	0.149 %	
γ	Temperature factor	-0.041 %/K	
$T_{\text{pv,ref}}$	Module temperature under standard test conditions	25 °C	
ϕ_C	Surface azimuth	14,0 °	
A	Surface area of one collector	1.675 m ²	
N_{pv}	Number of collectors	175,000	—○
$\eta_{\text{pv,conv}}$	Conversion efficiency	95 %	
ψ	Tilt angle	31 °	
ρ	Ground reflectance	0,2	—
$f_{\text{pv},I}$	Investment factor	250 €/collector	
$f_{\text{pv},C}$	Running cost factor	3.75 €/collector	
N_{turb}	Number of turbines	10	—○
$f_{\text{wind},I}$	Investment factor	1 Mio. €/turbine	
$f_{\text{wind},C}$	Running cost factor	15 ,000 €/turbine	

Table 9: Parameter settings for the sample power plant for Section 4.1. The sample plants parameters are taken from [7, 14, 6, 25, 13]. The indicated parameters are optimized in Section 4.2

4.1 Time horizon analysis

In the following section multiple linear programming strategies with different time horizons are compared to each other and to the baseline strategy.

In Figure 17 the results of the annual revenues of the linear programming strategies are presented. The best LP used the time horizon of 6 months with 7.73 Mio. € annual revenue whereas the weakest used 1 hour with 6.346 Mio. € as revenue. However, both LPs were better than the baseline strategy which generated 1.91 Mio. €. All results can be found in Table 11.

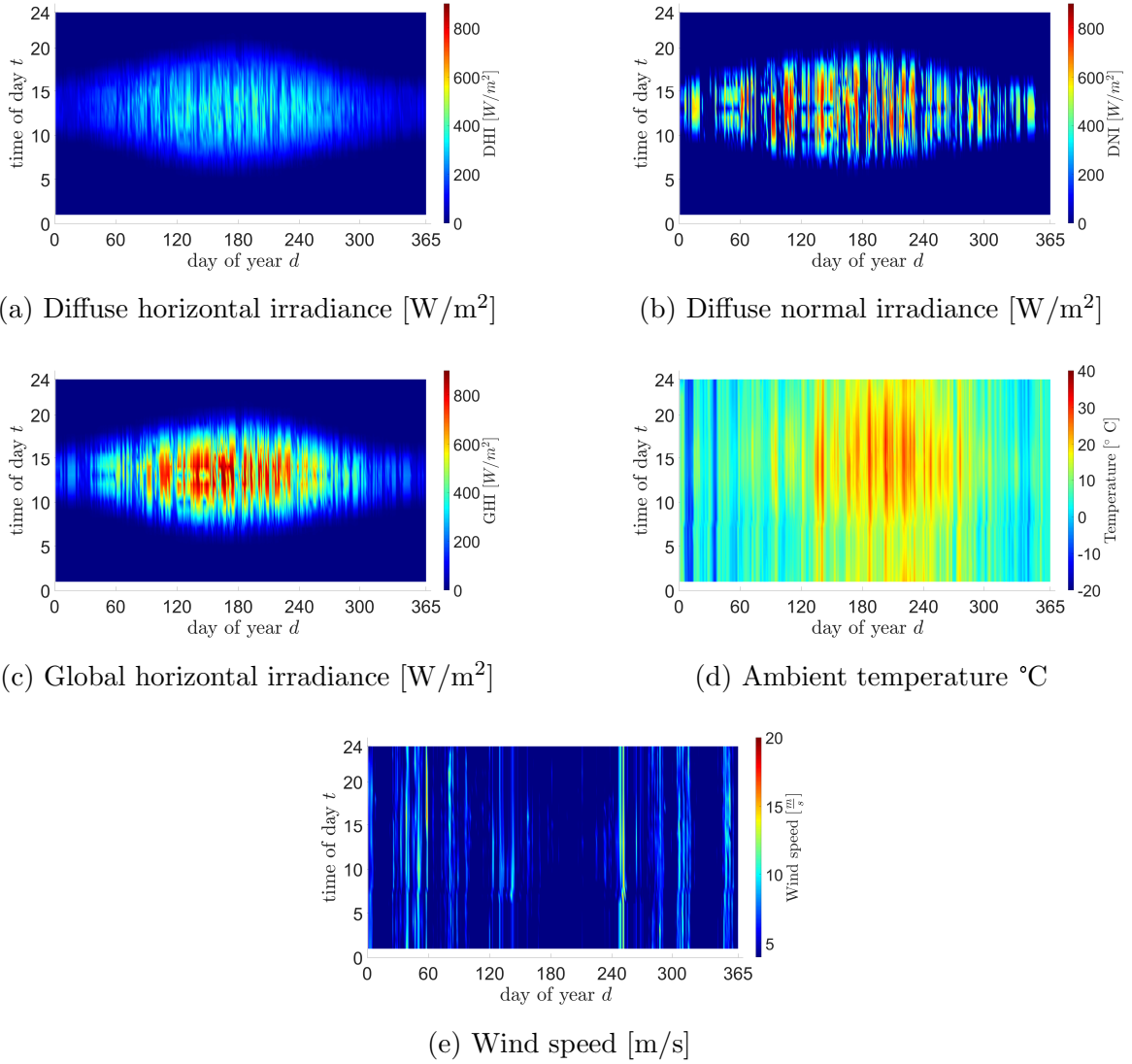


Figure 15: Different weather data is shown over one year for Aachen. This data is later used in the case studies. The color legend is on the right side of the respective figure.

Hour	Value [€]
1	19.77
2	17.37
3	32.01
4	28.78
5	31.79
6	42.00
7	45.01
8	45.03
9	45.00
10	45.00
11	45.07
12	44.32
13	45.69
14	46.01
15	45.00
16	45.00
17	46.06
18	48.00
19	47.08
20	45.09
21	43.95
22	42.04
23	40.15
24	34.07

Table 10: Values for Figure 16.

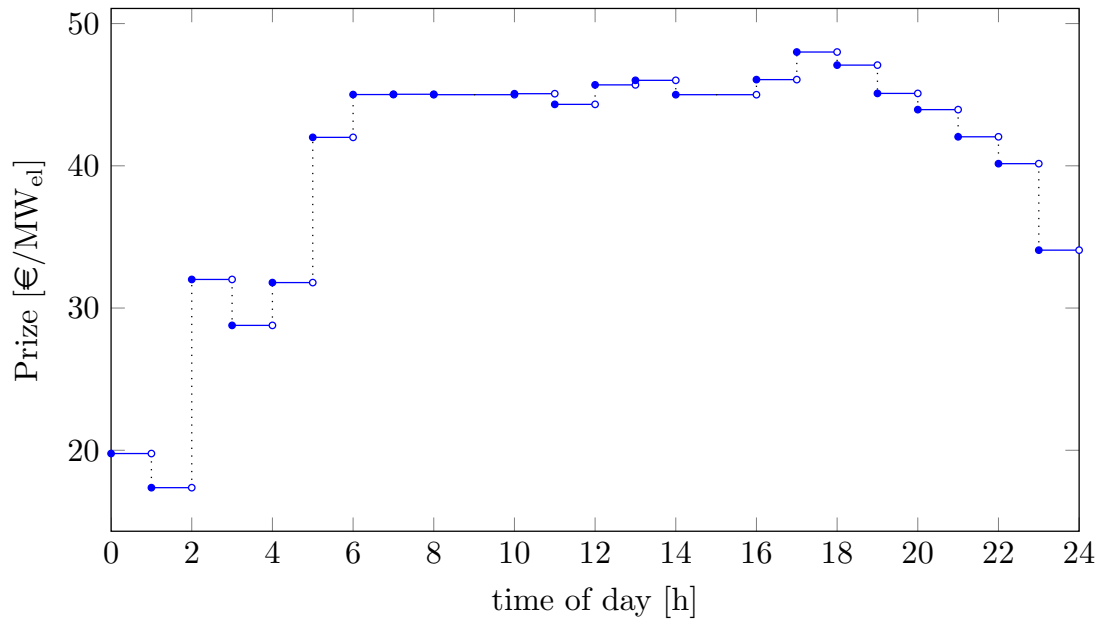


Figure 16: Hourly tariffs from the epex spot market [1]. The values are taken from the 19th November 2020. Table 10 lists the values.

Time horizon	Revenue [Mio. €]
1 hour	6 ,346
6 hours	7 ,187
12 hours	7 ,637
1 day	7 ,734
2 days	7 ,734
3 days	7 ,734
4 days	7 ,734
1 week	7 ,734
2 weeks	7 ,734
1 month	7 ,734
2 months	7 ,734
3 months	7 ,734
6 months	7 ,734

Table 11: All results from the experiments conducted to find the best time horizon.

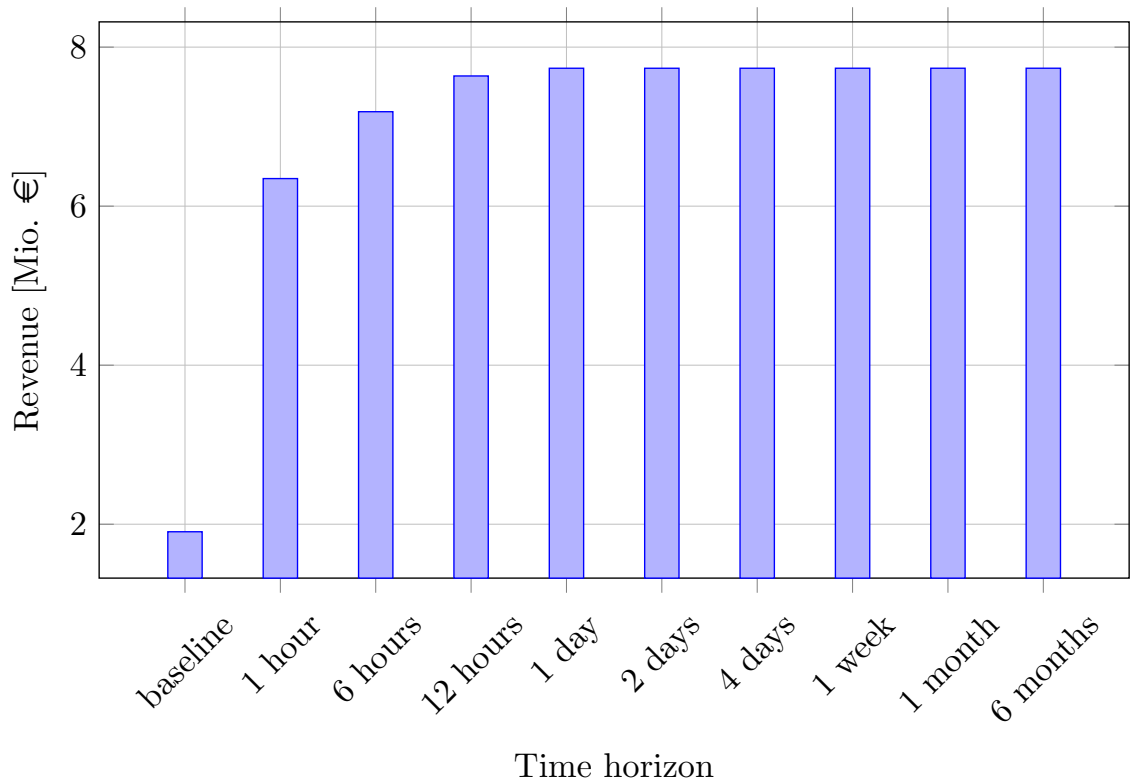


Figure 17: Annual revenue of the linear programming strategies depending on the various time horizons as well as the baseline strategy. All strategies used the sample virtual renewable power plant to control.

Furthermore, the LP with time horizon of 24 hours generates an annual revenue of 7.73 Mio. €, which is within 0.002% of the best LP with 6 months as time horizon. For all following case studies this work only uses the 24 hour time horizon as it is significantly faster to compute than the best LP.

4.2 Layout Optimization

The other optimization problem in this work is the layout optimization. Its goal is to find the best layout configuration so that the virtual renewable power plant is 100% self-sufficiently supplying its own power, while only having the minimal amount of investment and operational cost.

For each subsystem an optimization parameter and an interval is given in which the best value of this parameter is searched for:

- For the biogas system the optimization parameter is the storage capacity with the interval:

$$[Q_{\text{ch,min}}^{\text{bio,cap}}, Q_{\text{ch,max}}^{\text{bio,cap}}]$$

- For the hydro power plant the optimization parameter is the flowrate with the interval:

$$[\dot{V}_{\text{min}}^{\text{hydro}}, \dot{V}_{\text{max}}^{\text{hydro}}]$$

- For the pumped-storage hydropower system the optimization parameter is the storage capacity with the interval:

$$[Q_{\text{pot,min}}^{\text{pump,cap}}, Q_{\text{pot,max}}^{\text{pump,cap}}]$$

- For the power-to-gas system the optimization parameter is the storage capacity with the interval:

$$[Q_{\text{ch,min}}^{\text{gas,cap}}, Q_{\text{ch,max}}^{\text{gas,cap}}]$$

- For the photovoltaic power plant the optimization parameter is the number of collectors with the interval:

$$[N_{\text{pv,min}}, N_{\text{pv,max}}]$$

- For the wind power plant the optimization parameter is the number of turbines with the interval:

$$[N_{\text{turb,min}}, N_{\text{turb,max}}]$$

For the storage systems the highest suppliable and receivable power is defined in such a way that the storage can be charged and discharged in ten hours. This is done to reduce the complexity of the search and because the output and input power is rather restricted with storage systems. All configurations are controlled by the control strategy proposed in Section 3 and evaluated on the two equations (47), (48).

4.3 Autarky analysis for Herzogenrath

Herzogenrath is a city in the west of Germany close to Aachen with a population of 47,000. Therefore, the weather data introduced above closely resembles the weather in Herzogenrath as well. Furthermore, Herzogenrath does not have a river or water reservoirs for the pumped-storage, thus the following case study only focuses on the remaining subsystems.

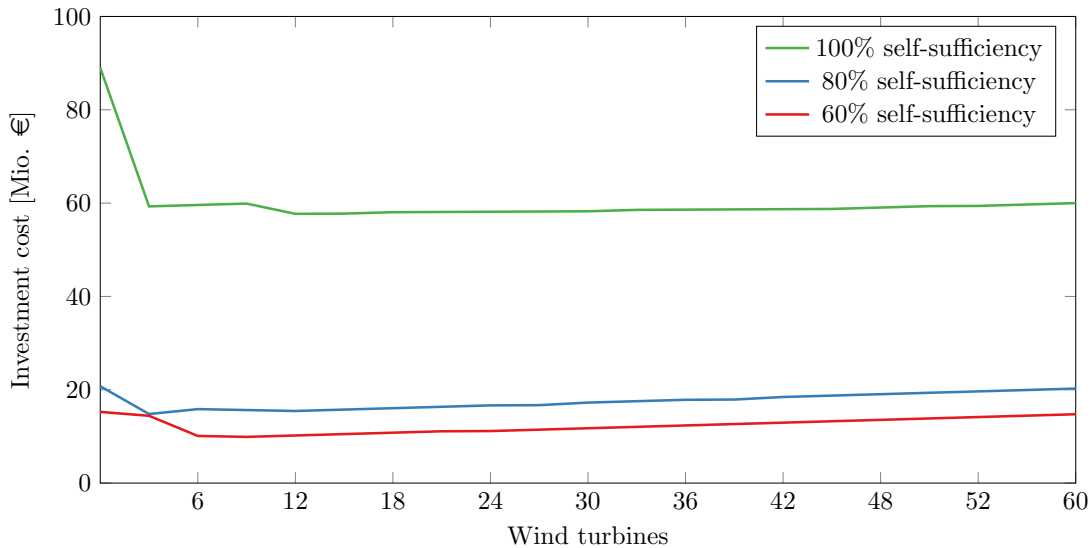


Figure 18: Investment comparison between different plant degrees of self-sufficiency.

As a first case study the best layout for three different degrees of self-sufficiency was searched. The desired self-sufficiency degrees were 60%, 80% and 100%. In this case study, the amount of wind turbines used in the virtual renewable plant were given and increased in steps of three until a limit of 60 was reached, while the remaining subsystems were optimized. The number of wind turbines were increased because the number of PV collectors and their resulting output can be optimized much more acutely.

In Figure 18 the results are shown. Both investment costs for 60% self-sufficiency and 80% self-sufficiency are noticeably lower than the investments for the 100% self-sufficient power plant. Consequently, the optimal configurations largely depend on the desired degree of self-sufficiency.

Furthermore, Figure 18 clearly shows, that a plant using no wind turbines for the complete self-sufficient supply is the worst configuration. Additionally, the optimum is reached when 12 turbines are used. From that point onwards, as shown by Table 12 as well, the investment costs only increase by 500,000 €, although wind turbines for the value of 3 Mio. € are added.

Tables 12, 13 and 14 show the evaluation results for every 10th percentage for the respective fraction of self-sufficiency as well as the respective configurations.

Percentage wind turbines	100% self-sufficiency					
	C_{Invest} [Mio. €]	LCOE [€ / MWh]	R^{el} [Mio. €]	$Q_{\text{ch}}^{\text{gas,cap}}$ [MW _{ch} h]	N_{pv} [Amount]	N_{turb} [Amount]
0	890.00	239.36	36.92	900	2 ,300 ,000	0
5	593.00	206.27	17.52	900	1 ,100 ,000	3
10	596.00	198.62	20.02	700	1 ,480 ,000	6
15	599.00	192.92	22.54	700	1 ,460 ,000	9
20	577.00	179.01	23.14	700	1 ,460 ,000	12
25	577.50	175.57	25.46	700	1 ,440 ,000	15
30	580.50	169.30	27.97	700	1 ,430 ,000	18
35	581.00	163.61	30.29	700	1 ,420 ,000	21
40	581.50	157.93	32.60	700	1 ,400 ,000	24
45	582.00	152.69	34.88	700	1 ,390 ,000	27
50	582.50	148.34	37.11	700	1 ,380 ,000	30
55	585.50	144.58	39.50	700	1 ,370 ,000	33
60	586.00	140.25	41.68	700	1 ,360 ,000	36
65	586.50	136.73	43.81	700	1 ,340 ,000	39
70	587.00	133.95	45.89	700	1 ,330 ,000	42
75	587.50	130.66	47.92	700	1 ,320 ,000	45
80	590.50	127.89	50.07	700	1 ,320 ,000	48
85	593.50	125.35	52.12	700	1 ,320 ,000	51
90	594.00	122.65	53.90	700	1 ,320 ,000	54
95	597.00	119.88	55.72	700	1 ,320 ,000	57
100	600.00	115.48	57.42	700	1 ,320 ,000	60

Table 12: Plant evaluations, configurations with investments, LCOE and revenue for the plants in Figure 18. The plants are restricted to achieve 100% self-sufficiency.

Percentage wind turbines	80% self-sufficiency					
	C_{Invest} [Mio. €]	LCOE [€ / MWh]	R^{el} [Mio. €]	$Q_{\text{ch}}^{\text{gas,cap}}$ [MW _{ch} h]	N_{pv} [Amount]	N_{turb} [Amount]
0	207.50	226.28	4.93	200	550 ,000	0
5	148.00	195.33	2.67	200	300 ,000	3
10	158.50	163.98	6.77	150	400 ,000	6
15	156.50	143.07	8.83	150	380 ,000	9
20	154.50	126.93	10.8	150	360 ,000	12
25	157.50	115.72	13.2	150	360 ,000	15
30	160.50	106.68	15.5	150	360 ,000	18
35	163.50	99.32	17.9	150	360 ,000	21
40	166.50	93.08	20.3	150	360 ,000	24
45	167.00	87.01	22.4	150	360 ,000	27
50	172.50	83.20	25.0	150	360 ,000	30
55	175.50	79.23	27.3	150	360 ,000	33
60	178.50	75.77	29.7	150	360 ,000	36
65	179.00	72.02	31.9	150	360 ,000	39
70	184.50	69.95	34.4	150	360 ,000	42
75	187.50	67.46	36.6	150	360 ,000	45
80	190.50	65.24	39.1	150	360 ,000	48
85	193.50	63.26	41.3	150	360 ,000	51
90	196.50	61.48	43.4	150	360 ,000	54
95	199.50	59.75	45.3	150	360 ,000	57
100	202.50	58.31	47.0	150	360 ,000	60

Table 13: Plant evaluations, configurations with investments, LCOE and revenue for the plants in Figure 18. The plants are restricted to achieve 80% self-sufficiency.

Percentage wind turbines	60% self-sufficiency					
	C_{Invest} [Mio. €]	LCOE [€ / MWh]	R^{el} [Mio. €]	$Q_{\text{ch}}^{\text{gas,cap}}$ [MW _{ch} h]	N_{pv} [Amount]	N_{turb} [Amount]
0	152.50	224.42	2.20	150	400 ,000	0
5	144.25	186.43	4.86	100	425 ,000	3
10	101.00	141.47	3.80	100	240 ,000	6
15	99.00	118.08	5.81	100	220 ,000	9
20	102.00	103.86	8.17	100	220 ,000	12
25	105.00	93.27	10.5	100	220 ,000	15
30	108.00	85.18	12.9	100	220 ,000	18
35	111.00	78.72	15.2	100	220 ,000	21
40	111.50	72.31	17.4	100	210 ,000	24
45	114.50	67.99	19.8	100	210 ,000	27
50	117.50	64.34	22.1	100	210 ,000	30
55	120.50	61.22	24.5	100	210 ,000	33
60	123.50	58.51	26.8	100	210 ,000	36
65	126.50	56.14	29.2	100	210 ,000	39
70	129.50	54.07	31.6	100	210 ,000	42
75	132.50	52.23	33.9	100	210 ,000	45
80	135.50	50.59	36.3	100	210 ,000	48
85	138.50	49.12	38.6	100	210 ,000	51
90	141.50	47.85	40.8	100	210 ,000	54
95	144.50	46.64	42.7	100	210 ,000	57
100	147.50	45.43	44.6	100	210 ,000	60

Table 14: Plant evaluations, configurations with investments, LCOE and revenue for the plants in Figure 18. The plants are restricted to achieve 60% self-sufficiency.

The levelized cost of energy was calculated for the above mentioned virtual renewable power plants as well. Figure 19 shows that the LCOE uniformly decreases for all shown self-sufficiency degrees, the more wind turbines are added to the virtual power plant.

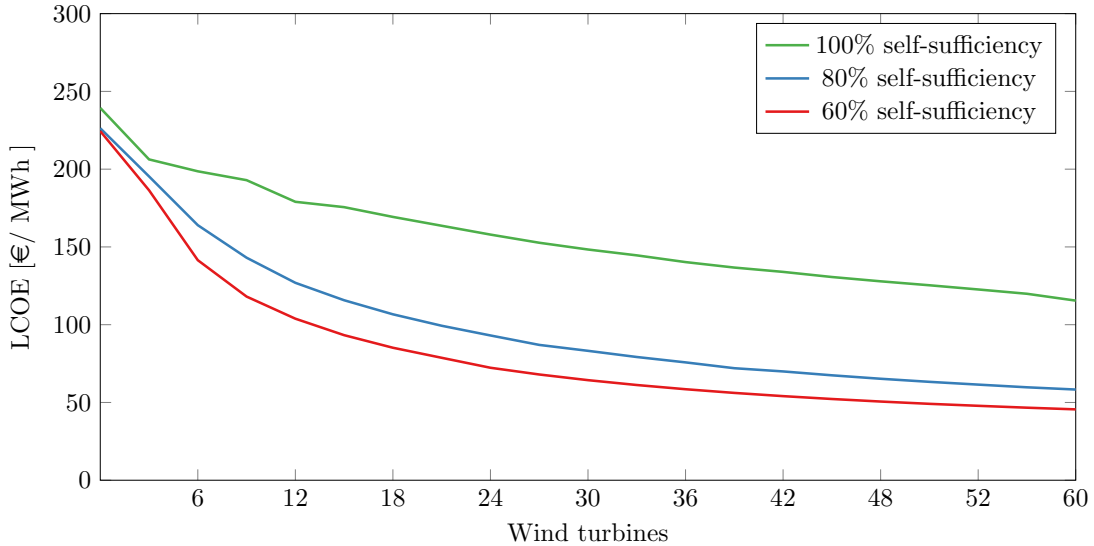


Figure 19: Levelized cost of energy comparison between different plant configurations.

Although some PV collectors are exchanged for wind turbines, as indicated by Table 12, Figure 20 shows a steady increase in revenue once wind turbines are used. Figure 20 however, also shows a large difference between the configuration using 0 and 3 wind turbines. This is caused by large differences in PV collectors, therefore over the course of one day, the virtual power plant has a lot of excess power. Figure 21 and Figure 22 show the stored energy in the power-to-gas storage and the sold power for the two plants. As can be seen, the power plant with no turbines has a storage that is nearly full throughout the whole year. Hence, if the sun is shining and a lot of power is added to the micro grid, the only use for it is to be sold as indicated by Figure 21. However, also shown in Figure 21 is that the stored energy for the plant using three turbines fluctuates more, therefore not as much power is available to be sold.

Going back to Figure 18, it can be seen that only using PV collectors is the worst configuration in order to achieve 100% self-sufficiency. Therefore, a second case study was performed to evaluate the investments for a virtual renewable power plant, that only uses wind turbines. Table 15 and Figure 23 compare the previously found optimal plant and the plant using no wind turbines to the power plant that only uses wind turbines. They show that using only wind turbines creates the necessity to also have storages with a combined capacity that is nearly four times larger than the other two plants need.

In Figure 24 the stored energy of the wind only virtual renewable power plant is shown. It is noticeable, that the storage is nearly empty around day 344 although it

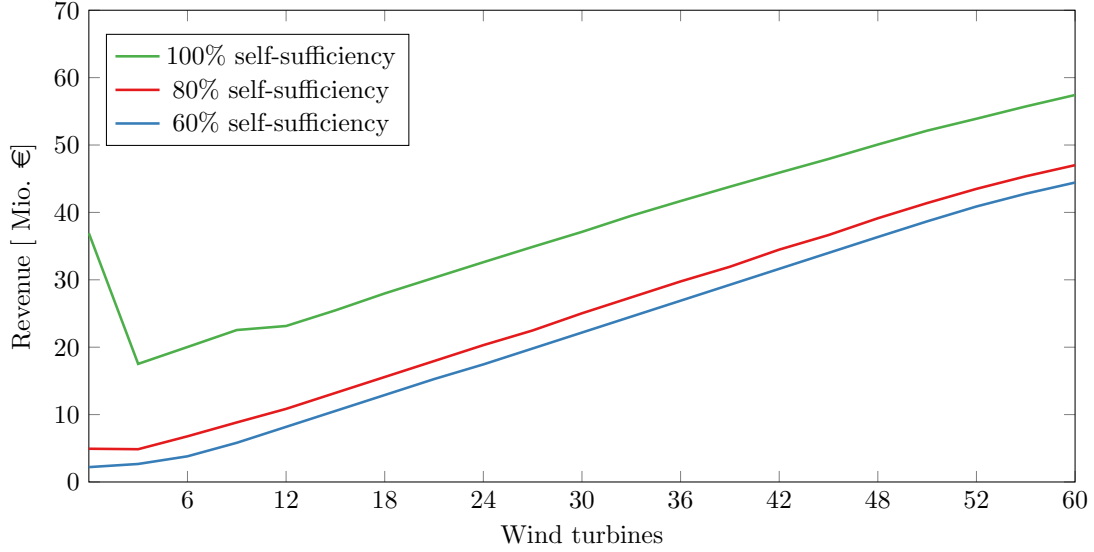


Figure 20: Revenue comparison between different plant configurations.

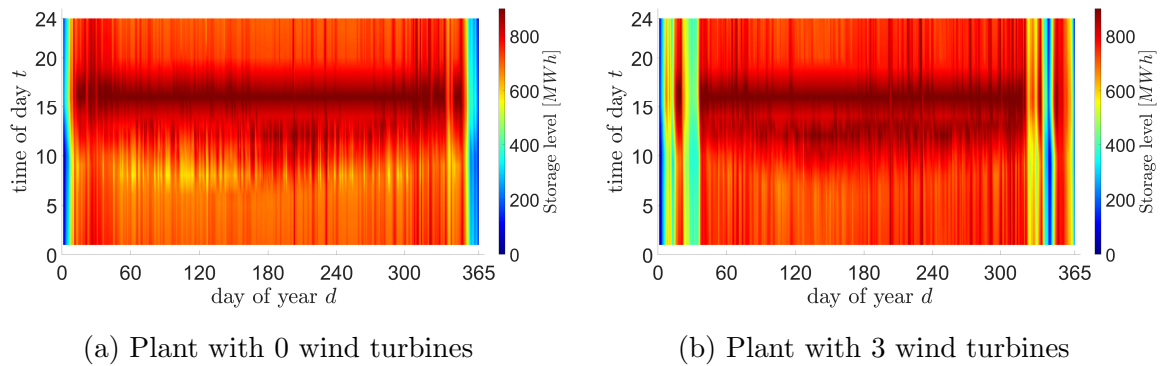


Figure 21: Comparison between the stored energies for the virtual renewable power plant with 0 and 3 wind turbines. The color legends are shown on the right side of the respective figure. They are chosen to range from zero to the capacity of the respective storage.

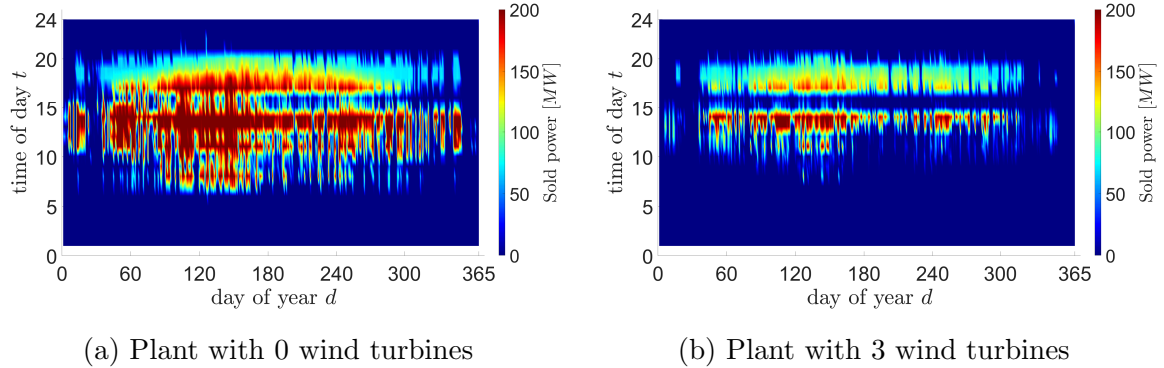


Figure 22: Comparison between the sold power for the virtual renewable power plant with 0 and 3 wind turbines. The color legends are shown on the right side of the respective figure.

Layout Parameter	Quantities		
	wind & pv	only pv	only wind
Biogas capacity [MW _{ch} h]	0	0	50
Power-to-gas capacity [MW _{ch} h]	900	900	3200
PV collectors	2 ,000 ,000	2 ,300 ,000	0
Wind turbines	12	0	50
C_{Invest} [Mio. €]	577.0	890.0	1 ,187 .5

Table 15: Layout configuration for the complete self-sufficient virtual renewable power plant using either wind and solar power plant and both.

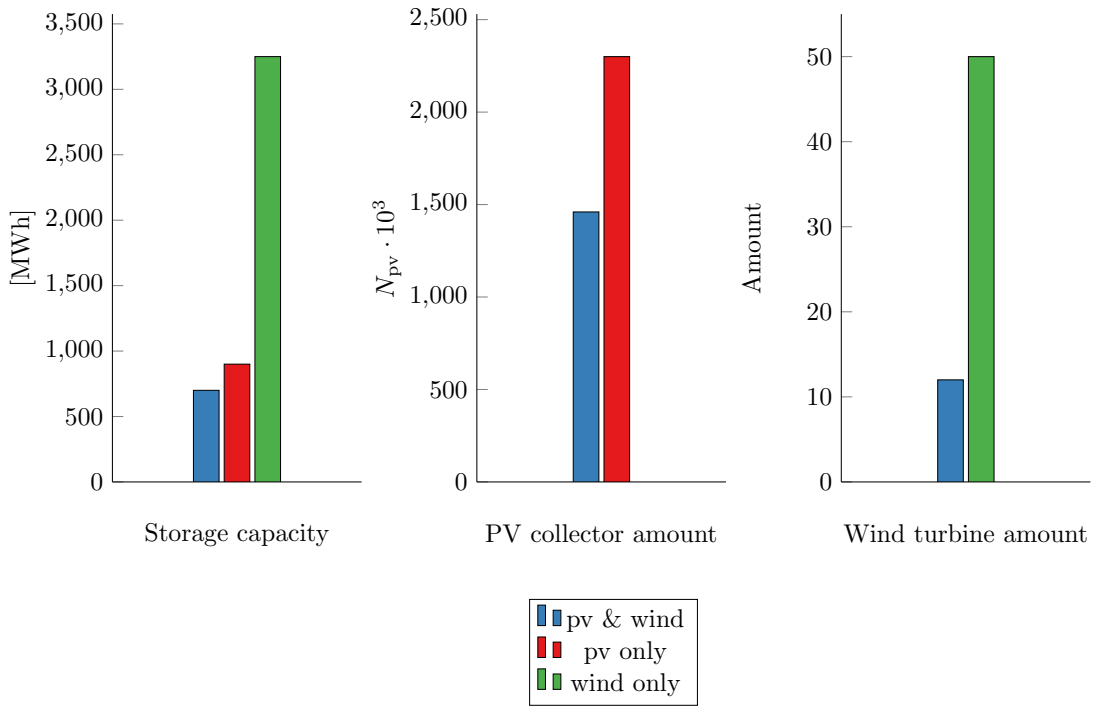


Figure 23: Comparison of the configurations for the three different power plants. The plant shown in red only uses the PV plant, the blue one the only wind power plant. Finally, the virtual renewable power plant shown in green uses both renewable power plants.

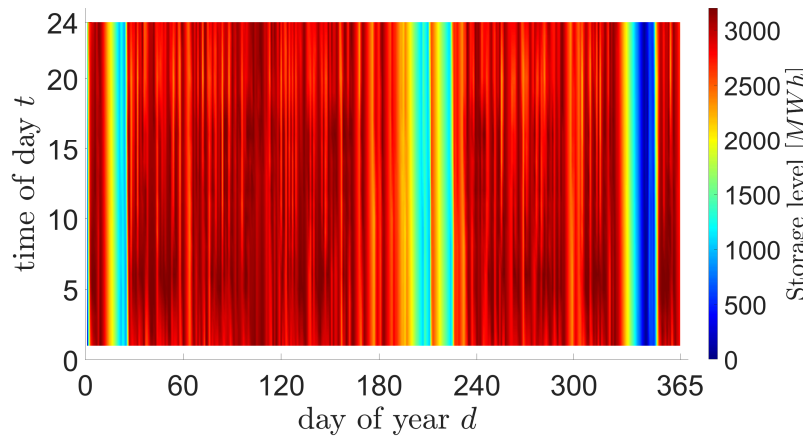


Figure 24: Stored energy of the power-to-gas system for the wind only virtual renewable power plant. The color legends are shown on the right side of the respective figure.

has a capacity of $3250 \text{ MW}_{\text{ch}}\text{h}$, which is full almost the entire year. In reference to Figure 15 this phenomenon can be explained. There are large intervals throughout the year, in which the wind speed is not high enough to be converted into electricity. In order to achieve 100% self-sufficient power supply with only wind turbines the power plant has to compensate for that only using the available stored energy.

4.4 Autarky analysis for Herzogenrath using hydro subsystems

As mentioned before Herzogenrath does not have the ability to harness the hydro power plant or the pumped-storage hydropower. However, in this section as a case study, Herzogenrath will be virtually extended with these subsystems. It is assumed, that a pumped-storage can be built with only 20 Mio. €. This would be possible if two lakes already existed close to Herzogenrath. The pumped-storage would have a capacity of $500 \text{ MW}_{\text{el}}\text{h}$. Furthermore, the micro grid of Herzogenrath is extended with a hydro power plant which has a peak output power of about 9 MW_{el} . This plant is assumed to be built with 10 Mio. €. The flowrates that are used as input were taken from Pegelonline³, they represent the river Main near Würzburg. A representation can be seen in Figure 25

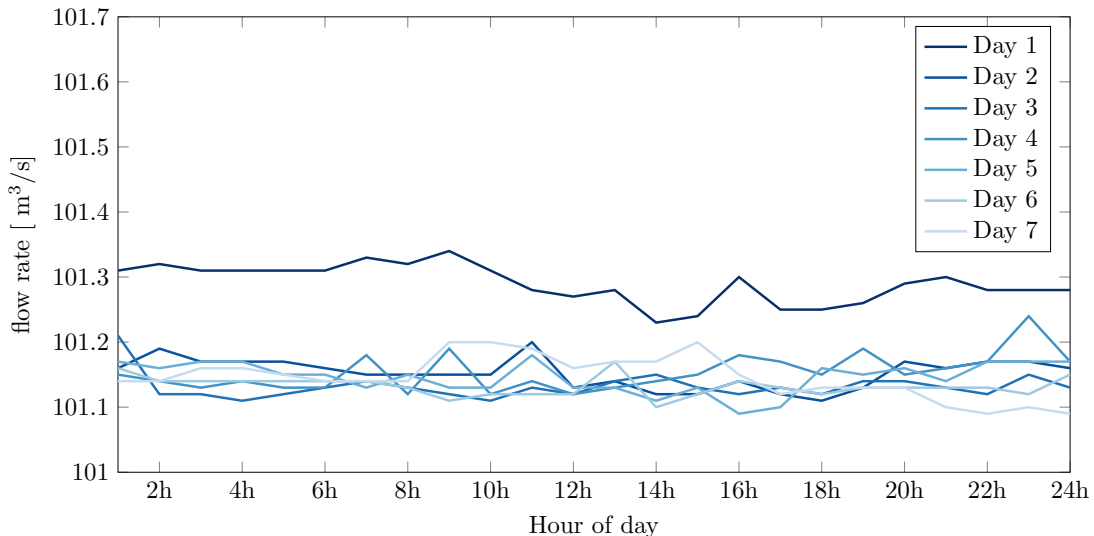


Figure 25: Flowrates for the hydro power plant of the river Main near Würzburg. The 7 day data is extrapolated over one year.

All parameters for the two subsystems are shown in Table 16.

³<https://www.pegelonline.wsv.de/gast/start>

Parameter		Value
$Q_{\text{pot}}^{\text{pump,cap}}$	Pumped-storage capacity	500MW _{ch} h
$\eta_{\text{pump,char}}$	Pumped-storage charging efficiency	80 %
$\eta_{\text{pump,gen}}$	Pumped-storage discharging efficiency	80 %
$P_{\text{el}}^{\text{pump,sup,max}}$	Pumped-storage highest suppliable power	50MW _{el}
$P_{\text{el}}^{\text{pump,rec,max}}$	Pumped-storage highest receivable power	50MW _{el}
ΔH_{pump}	Pumped-storage hydraulic head	50m
ΔH_{hydro}	Hydro plant hydraulic head	50 m
η_{hydro}	Hydro plant efficiency	80 %

Table 16: Parameters for the hydro power plant and the pumped-storage.

In this case study a layout configuration for 100% self-sufficiency is searched for. The investments, LCOE and revenue are shown in Figure 26, 27 and 28 are to against the before mentioned results. Furthermore, the amount of wind turbines was determined as before.

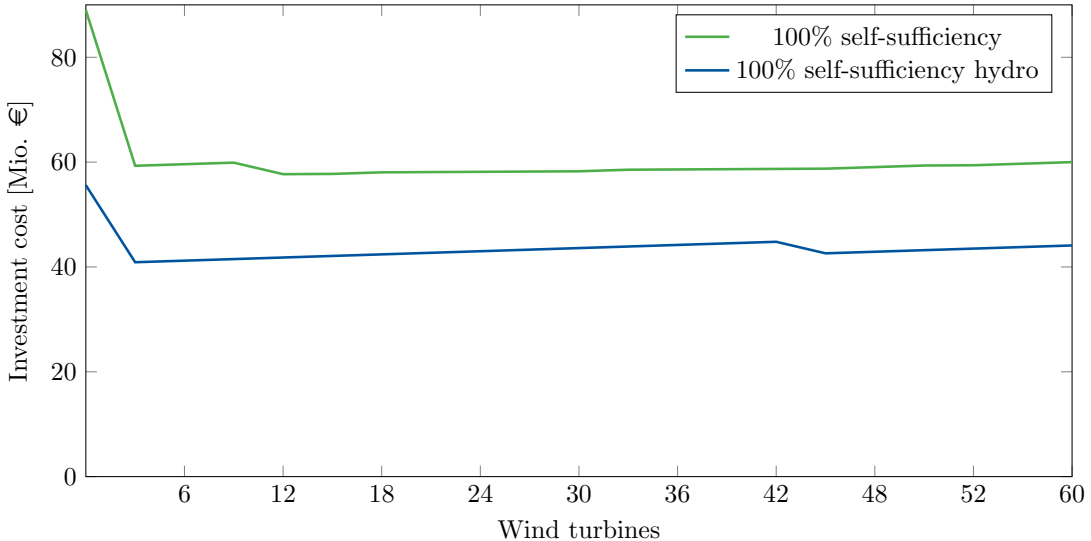


Figure 26: Investments for the hydro extension plant compared to the previous findings.

As can be seen every evaluation on the hydro extension plant is by far better than the previous completely self-sufficient power plant which uses both PV and wind power plants. Considering the flowrates visualized in Figure 25 the hydro power plant consistently outputs electricity, which is a huge benefit. In Table 17 the most optimal configuration regarding investment costs is compared against the optimal configuration found in Section 4.3. Although the needed power-to-gas capacity is rather high

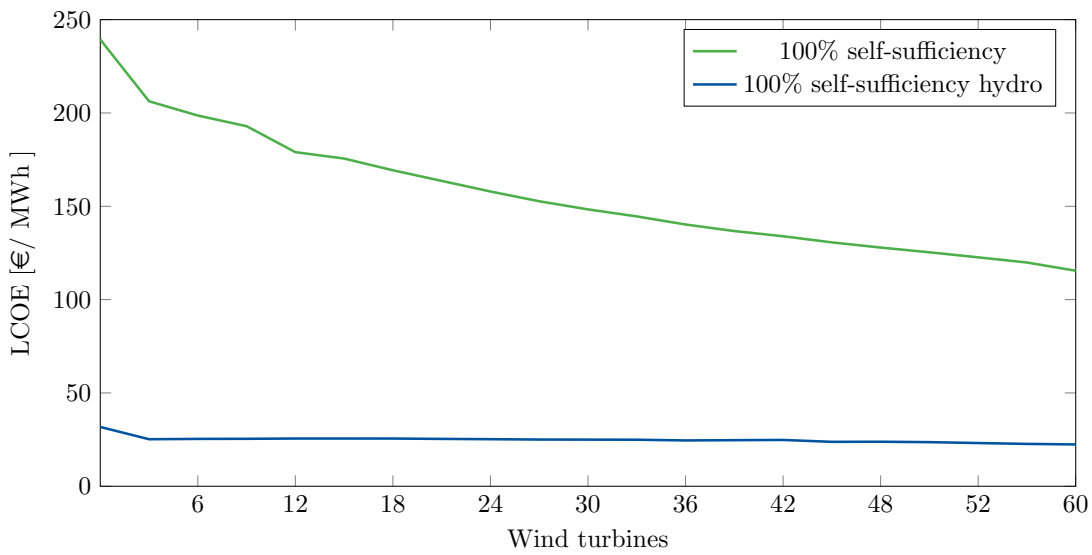


Figure 27: LCOE for the hydro extension plant compared to the previous findings.

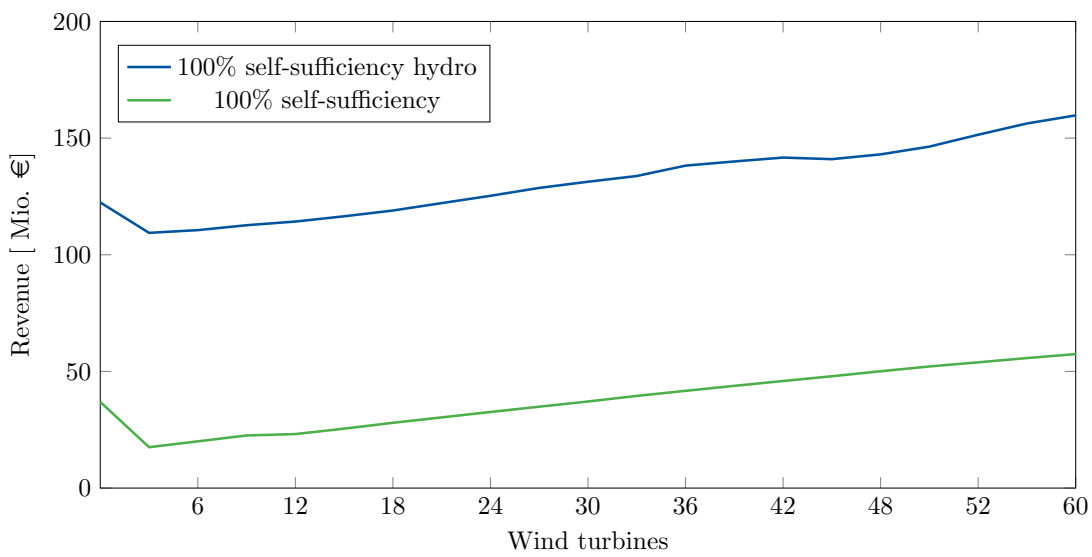


Figure 28: Revenue for the hydro extension plant compared to the previous findings.

Layout parameter	units	hydro extension plant	previous optimum
Biogas capacity	MW _{ch} h	0	0
Power-to-gas capacity	MW _{ch} h	600	0
Pumped-storage capacity	MW _{el} h	500	900
PV collectors	Amount	700 ,000	1 ,460 ,000
Wind turbines	Amount	3	12
C_{Invest}	Mio. €	409.0	577.0

Table 17: Layout configuration for the complete self-sufficient virtual renewable power plant using wind, solar and hydro power plant.

the investment costs are only 10 Mio. € on top of investment costs for the hydro subsystems.

Figure 29 shows a visual representation of Table 17.
The presented case studies show that it is most beneficial for the complete self-sufficient power supply for counties, using virtual renewable power plants, to harvest as much renewable energy sources as are available.

4.5 Discussion of the results

For a virtual renewable power plant a LP control strategy using a 24 hour time horizon yields nearly the same result as using larger time horizons, see Table 11. Even with a time horizon of 1 hour the LP control strategy already outperforms the baseline strategy by far. The baseline strategy was designed preferring storage over selling electricity. However, since the LP control strategies objective function is the electric revenue (56), the difference is explained. Nevertheless, the LP control strategy should clearly be preferred because of the huge difference in revenue as a control strategy for the layout optimization.

The optimal layout of a virtual renewable power plant depends on the desired degree of self-sufficiency. Furthermore, it is shown, that if PV and wind power plants are able to be used, the optimal solution with regards to the investment cost is to use both, as opposed to using only either one. Additionally, Sections 4.3 and 4.4 conclude that using as much renewable energy sources as possible to achieve complete self-sufficient power supply is the most beneficial for all presented evaluation methods.

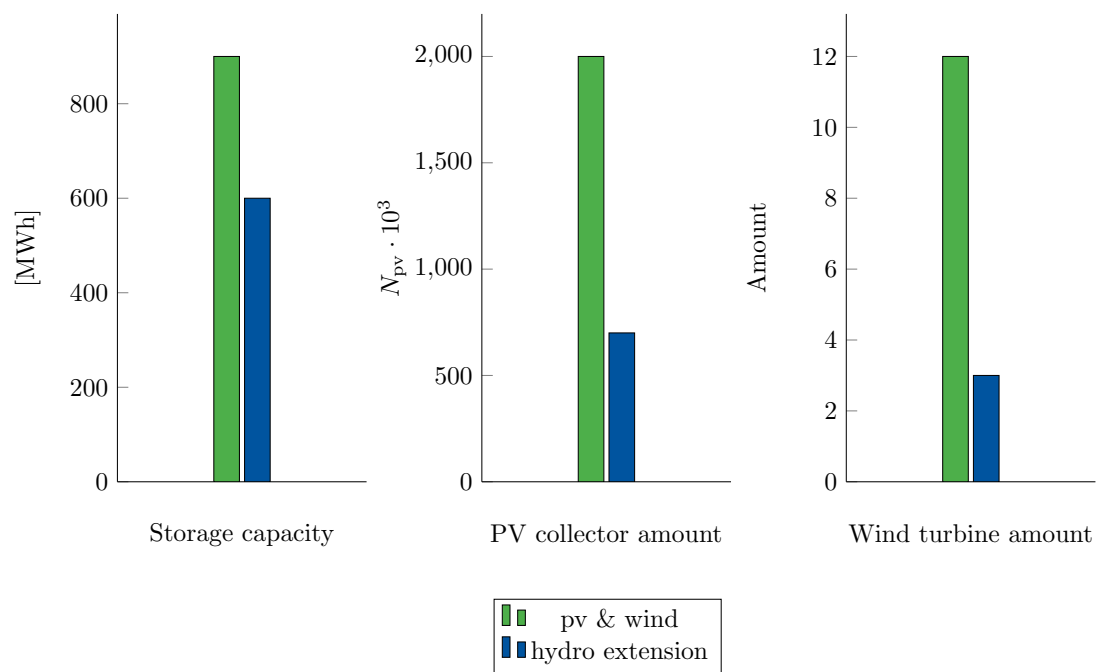


Figure 29: Comparison of the configurations for the power plant using hydro power as well as the wind and PV plants. The other plant only uses the PV and wind power plant.

5 Conclusion and Future Work

In this work a control strategy using linear programming for a virtual renewable power plant is developed. This type of virtual power plant uses only renewable power plants as electricity production. Furthermore, the plant builds a micro electricity grid, in which the main consumer is a county area. The goal of the virtual renewable power plant is to supply completely self-sufficiently the county area with electricity. The future electricity tariff and future weather conditions are factored into a linear programming control strategy. Different time horizons for this LP control strategy are evaluated and compared against a non-LP baseline strategy. In a case study it is shown that the LP control strategy outperforms the baseline strategy by far. In addition, it is shown that a LP control strategy with a time horizon of 24 hours yield the same results as the ones using larger time horizons.

For the layout optimization case studies were conducted with Herzogenrath as county area. The result is that the layout optimization is able to find virtual renewable power plant configurations for given degrees of self-sufficiency. Additionally, it is shown, that the most optimal power plant configuration to meet 100% requires less than 600 Mio. € and only using 12 wind turbines. Furthermore, this work presents that harvesting all available sources of renewable energy is the most beneficial, regarding investment costs, in order to achieve complete self-sufficient power supply for counties.

Future work The models of the power plants and storage systems are linear, which is only a rough representation of reality. This should be extended in order to study real life virtual renewable power plant usage.

Furthermore, the automotive market experiences an upheaval towards more climate friendly electric vehicles. Those can be utilized as volatile storage units at night or when the owner is at the workplace.

Besides, the economic model could be extended to consider the reduction of necessary carbon dioxide taxes or the local value added.

Acknowledgments

I would first like to thank my thesis advisor Dr. Pascal Richter for all the guidance and support during the development of this thesis. I appreciate the continuous patience and revisions during this time.

Furthermore, I thank all my friends who supported me during my time as a bachelor student.

I am deeply grateful for my family, especially my parents without whom I would never have come this far.

Lastly, I thank my grandmother for all her guidance, who unfortunately cannot see me graduate.

Thank you.

References

- [1] Auction > intraday > 60min > ch > 20 november 2020. URL https://www.epexspot.com/en/market-data?market_area=CH&trading_date=2020-11-19&delivery_date=2020-11-20&underlying_year=&modality=Auction&sub_modality=Intraday&product=60&data_mode=graph&period=.
- [2] Brandi A Antal. Pumped Storage Hydropower: A Technical Review in the area of Hydrologic and Hydraulic Engineering. Technical Report May, 2004.
- [3] Eduardo F Camacho and Manuel Berenguel. Control of solar energy systems. *IFAC proceedings volumes*, 45(15):848–855, 2012.
- [4] Luigi R Cirocco, Martin Belusko, Frank Bruno, John Boland, and Peter Pudney. Controlling stored energy in a concentrating solar thermal power plant to maximise revenue. *IET Renewable Power Generation*, 9(4):379–388, 2015.
- [5] Stella Coumbassa. Optimal storage strategy for hybrid concentrated solar power - photovoltaic plants. Master’s thesis, RWTH Aachen University, 11 2019.
- [6] Dorothee dos Santos. Power-to-gas: Potenziale, grenzen und geschäftsmodelle, 2020. URL <https://www.euwid-energie.de/dossier-power-to-gas-fuer-die-energiewende/>.
- [7] Fachagentur Nachwachsende Rohstoffe e. V. (FNR) and Landwirtschaft und Verbraucherschutz (BMELV) Bundesministerium für Ernährung. Biogas Basisdaten Deutschland. *Agrartechnik*, 2008.
- [8] Andrés Feijóo, José Luis Pazos, and Daniel Villanueva. Conventional Asynchronous Wind Turbine Models. *International Journal of Energy Engineering - IJEE*, 3(6):269–278, 2013.
- [9] NOAA National Centers for Environmental Information. State of the climate: Global climate report for annual 2019, 2020. URL <https://www.ncdc.noaa.gov/sotc/global/201913>.
- [10] Bundesministerium für Wirtschaft und Energie. Kohleausstieg und strukturwandel, 2019. URL <https://www.bmwi.de/Redaktion/DE/Artikel/Wirtschaft/kohleausstieg-und-strukturwandel.html>.
- [11] Marco Giuntoli and Davide Poli. Optimized thermal and electrical scheduling of a large scale virtual power plant in the presence of energy storages. *IEEE Transactions on Smart Grid*, 4(2):942–955, 2013.
- [12] Nikos D Hatzigergiou. Special issue on microgrids and energy management. *European Transactions on Electrical Power*, 21(2):1139–1141, 2011.

- [13] Erich Hau. *Windkraftanlagen: Grundlagen. Technik. Einsatz. Wirtschaftlichkeit.* Springer-Verlag, 2017.
- [14] Das Internationale Wirtschaftsforum Regenerative Energien (IWR). Checkliste: Planung und leitfaden zum bau einer biogas-anlage. URL <http://www.iwr.de/bio/biogas/Checkliste-Biogas-Anlage.html>.
- [15] Mareike Jentsch, Tobias Trost, and Michael Sterner. Optimal use of power-to-gas energy storage systems in an 85% renewable energy scenario. *Energy Procedia*, 46 (0):254–261, 2014.
- [16] Thomas R Karl and Kevin E Trenberth. Modern global climate change. *science*, 302(5651):1719–1723, 2003.
- [17] Igor Kuzle, Marko Zdrilić, and Hrvoje Pandžić. Virtual power plant dispatch optimization using linear programming. In *2011 10th International Conference on Environment and Electrical Engineering*, pages 1–4. IEEE, 2011.
- [18] George Cristian Lazaroiu and Mariacristina Roscia. Definition methodology for the smart cities model. *Energy*, 47(1):326–332, 2012.
- [19] Pio Lombardi, Michal Powalko, and Krzysztof Rudion. Optimal operation of a virtual power plant. In *2009 IEEE Power & Energy Society General Meeting*, pages 1–6. IEEE, 2009.
- [20] BT Nijaguna. *Biogas technology*. New Age International, 2006.
- [21] Shafiqur Rehman, Luai M Al-Hadhrami, and Md Mahbub Alam. Pumped hydro energy storage system: A technological review. *Renewable and Sustainable Energy Reviews*, 44:586–598, 2015.
- [22] Kathryn Mersmann (USRA): Lead Producer Ellen T. Gray (ADNET): Lead Writer Patrick Lynch (NASA/GSFC): Lead Public Affairs Officer Gavin A. Schmidt (NASA/GSFC GISS): Lead Scientist. 2018 was the fourth hottest year on record, 2019. URL <https://svs.gsfc.nasa.gov/13142>.
- [23] Marko Zdrilić, Hrvoje Pandžić, and Igor Kuzle. The mixed-integer linear optimization model of virtual power plant operation. In *2011 8th International Conference on the European Energy Market (EEM)*, pages 467–471. IEEE, 2011.
- [24] Jan Martin Zepter, Tatiana Gabderakhmanova, Karl Maribo Andreasen, Knud Boesgaard, and Mattia Marinelli. Biogas plant modelling for flexibility provision in the power system of bornholm island. In *2020 Proceedings of the 55th International Universities Power Engineering Conference (UPEC)*, pages 1–6, 2020.
- [25] Rongrong Zhai, Ying Chen, Hongtao Liu, Hao Wu, Yongping Yang, and Mohammad O. Hamdan. Optimal Design Method of a Hybrid CSP-PV Plant Based on Genetic Algorithm Considering the Operation Strategy. *International Journal of Photoenergy*, 2018, 2018. ISSN 1687529X. doi: 10.1155/2018/8380276.